

VOLUME 9 NUMBER 1 JUNE 2024

ISSN: 2528-1682, e-ISSN: 2527-9165

























Published by:

Department of Informatics

UIN Sunan Gunung Djati Bandung

SERTIFIKAT

Direktorat Jenderal Penguatan Riset dan Pengembangan, Kementerian Riset, Teknologi dan Pendidikan Tinggi

TERAKREDITASI



Kutipan dari Keputusan Direktur Jenderal Penguatan Riset dan Pengembangan Kementerian Riset, Teknologi dan Pendidikan Tinggi F SK lik Indonesia Nomor 36/E/KPT/2019

Peringkat Akreditasi Jurnal Ilmiah Periode VII Tahun 2019

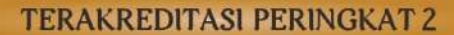
Nama Jurnal Ilmiah

JOIN (Jurnal Online Informatika)

E-ISSN: 25279165

Penerbit: Jurusan Teknik Informatika, UIN Sunan Gunung Djati Bandung

Ditetapkan Sebagai Jurnal Ilmiah



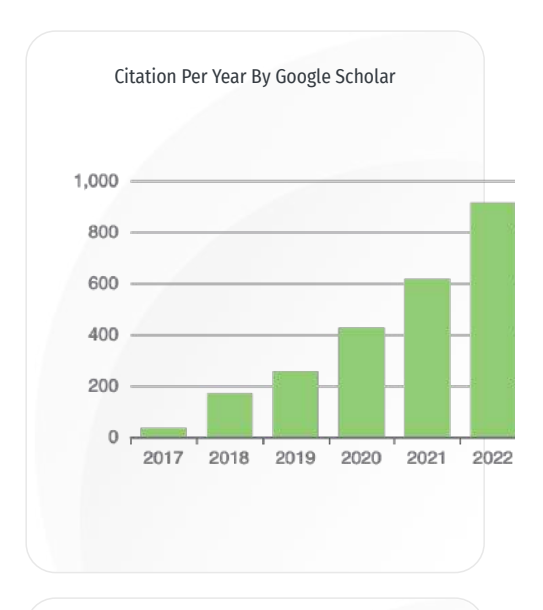
Akreditasi Berlaku Selama 5 (lima) Tahun, Yaitu Volume 4 Nomor 1 Tahun 2019 sampai Volume 8 Nomor 2 Tahun 2023

Direktur Jenderal Penguatan Riset dan Pengembangan

NIP. 195912171984021001



Get More with
SINTA Insight
Go to Insight



Journal By Google Scholar			
	All	Since 2020	
Citation	2927	2863	
h-index	25	25	
i10-index	58	58	

Search...

The Impact of Online Reviews to Predict The Number of International Tourists

<u>Department of Informatics, UIN Sunan Gunung Djati Bandung</u>

<u>Informatika) Vol 10 No 1 (2025) 77-92</u>

□ 2025 □ DOI: 10.15575/join.v10i1.1409 ○ Accred : Sinta 2

<u>Application of Self-Organizing Map and K-Means to Cluster Bandwidth Usage</u> <u>Patterns in Campus Environment</u>

<u>Department of Informatics, UIN Sunan Gunung Djati Bandung</u>

<u>Informatika) Vol 10 No 1 (2025) 66-76</u>

□ 2025 □ DOI: 10.15575/join.v10i1.1438 ○ Accred : Sinta 2

<u>Study of the Application of Text Augmentation with Paraphrasing to Overcome</u> <u>Imbalanced Data in Indonesian Text Classification</u>

Department of Informatics, UIN Sunan Gunung Djati Bandung
Informatika) Vol 10 No 1 (2025) 132-142

<u>□ 2025</u> <u>□ DOI: 10.15575/join.v10i1.1472</u> <u>○ Accred : Sinta 2</u>

Road Damage Detection Using YOLOv7 with Cluster Weighted Distance-IoU NMS

<u>Department of Informatics, UIN Sunan Gunung Djati Bandung</u> <u>Informatika) Vol 10 No 1 (2025) 122-131</u>

□ 2025 □ DOI: 10.15575/join.v10i1.1481 ○ Accred : Sinta 2

JOIN (Jurnal Online

JOIN (Jurnal Online

<u>LLM-Based Information Retrieval for Disease Detection Using Semantic Similarity</u>

<u>Department of Informatics, UIN Sunan Gunung Djati Bandung</u> Informatika) Vol 10 No 1 (2025) 32-41

□ 2025 □ DOI: 10.15575/join.v10i1.1486 ○ Accred : Sinta 2

<u>Modality-based Modeling with Data Balancing and Dimensionality Reduction for Early Stunting Detection</u>

<u>Department of Informatics, UIN Sunan Gunung Djati Bandung</u>

<u>Informatika) Vol 10 No 1 (2025) 53-65</u>

<u>□ 2025</u> <u>□ DOI: 10.15575/join.v10i1.1495</u> <u>○ Accred : Sinta 2</u>

<u>Adoption of Artificial Intelligence and Digital Resources among Academicians of Islamic Higher Education Institutions in Indonesia</u>

<u>Department of Informatics, UIN Sunan Gunung Djati Bandung</u>

<u>Informatika) Vol 10 No 1 (2025) 42-52</u>

<u>□ 2025</u> <u>□ DOI: 10.15575/join.v10i1.1549</u> <u>○ Accred : Sinta 2</u>

<u>Pyramid Quantum Neural Network Based Resource Allocation with IoT: A Deep Learning Method</u>

<u>Department of Informatics, UIN Sunan Gunung Djati Bandung</u>

<u>Informatika) Vol 10 No 1 (2025) 143-152</u>

□ 2025 □ DOI: 10.15575/join.v10i1.1578 ○ Accred : Sinta 2

<u>Performance Comparative Study of Machine Learning Classification Algorithms for</u> <u>Food Insecurity Experience by Households in West Java</u>

<u>Department of Informatics, UIN Sunan Gunung Djati Bandung</u>

<u>Informatika) Vol 9 No 1 (2024) 128-137</u>

□ 2024 □ DOI: 10.15575/join.v9i1.1012 ○ Accred : Sinta 2

Enchancing Lung Disease Classification through K-Means Clustering, Chan-Vese Segmentation, and Canny Edge Detection on X-Ray Segmented Images

<u>Department of Informatics, UIN Sunan Gunung Djati Bandung</u>

<u>Informatika) Vol 9 No 1 (2024) 89-99</u>

<u>□ 2024</u> <u>□ DOI: 10.15575/join.v9i1.1178</u> <u>○ Accred : Sinta 2</u>

 Previous
 1
 2
 3
 4
 5
 Next

Page 3 of 48 | Total Records 479



HOME / ARCHIVES / Vol. 9 No. 1 (2024)

Vol. 9 No. 1 (2024)



All articles in this issue (15 original research articles) were authored/co-authored by 7 (seven) countries (Indonesia, Malaysia, Egypt, Iraq, United States, India, and Ghana).

DOI: https://doi.org/10.15575/join.v9i1

PUBLISHED: 2024-04-23

ARTICLE

A Comparison of Ryu and Pox Controllers: A Parallel Implementation

Muhammad Ikhwananda Rizaldi, Department of Informatics, University of Muhammadiyah Malang, Indonesia Elsa Annas Sonia Yusuf, Department of Informatics, University of Muhammadiyah Malang, Indonesia Denar Regata Akbi, Department of Informatics, University of Muhammadiyah Malang, Indonesia Wildan Suharso, Department of Informatics, University of Muhammadiyah Malang, Indonesia

DOI: 10.15575/join.v9i1.1181 | Abstract View: 751 | PDF downloads: 619

△ PDF

1-9

Modeling Face Detection Application Using Convolutional Neural Network and Face-API for Effective and Efficient Online Attendance Tracking

Carles Juliandy, Department of Information Technology, Universitas Mikroskil, Indonesia Ng Poi Wong, Department Computer Science, Universitas Mikroskil, Indonesia Darwin, Department Computer Science, Universitas Mikroskil, Indonesia

dol > DOI : 10.15575/join.v9i1.1203 ldl Abstract View : 936 № PDF downloads: 781

Deep Learning Based LSTM Model for Predicting the Number of Passengers for Public Transport Bus Operators

Joko Siswanto, Politeknik Keselamatan Transportasi Jalan; Faculty of Information Technology, Satya Wacana Christian

18-2
University, Indonesia

https://orcid.org/0000-0003-3795-2155

Danny Manongga, Faculty of Information Technology, Satya Wacana Christian University, Indonesia Irwan Sembiring, Faculty of Information Technology, Satya Wacana Christian University, Indonesia Sutarto Wijono, Faculty of Information Technology, Satya Wacana Christian University, Indonesia

doi > DOI : 10.15575/join.v9i1.1245 Lttl Abstract View : 1406 L PDF downloads: 707

🛭 PDF

MAKE A SUBMISSION

ACCREDITED



EDITORIAL TEAM

CITEDNESS IN SCOPUS

PEER REVIEW PROCESS

FOCUS AND SCOPE

PUBLICATION ETHICS

AUTHOR GUIDELINES

AUTHOR FEES

DATA SHARING POLICY

REVENUE SOURCES

ADVERTISING POLICY

DIRECT MARKETING

RETRACTION-CORRECTIONS

COPYRIGHT NOTICE

PLAGIARISM CHECK

REFERENCES MANAGEMENT

JOURNAL HISTORY

TOOLS



Analysis of Data and Feature Processing on Stroke Prediction using Wide Range Machine Learning Model

Untari Novia Wisesty, School of Computing, Telkom University, Bandung, Indonesia Tjokorda Agung Budi Wirayuda, School of Computing, Telkom University, Bandung, Indonesia Febryanti Sthevanie, School of Computing, Telkom University, Bandung, Indonesia Rita Rismala, School of Computing, Telkom University, Bandung, Indonesia

doi> DOI: 10.15575/join.v9i1.1249 Ltd Abstract View: 1211 L PDF downloads: 650

☑ PDF

Case Study in Network Security System Using Random Port Knocking Method on The Principles of Availability, **Confidentiality and Integrity**

Tati Ernawati, Informatics Engineering Study Program, TEDC Bandung Polytechnic, Indonesia https://orcid.org/0000-0002-0108-1098

₫ 41-51

Idham Kholid, Informatics Engineering Study Program, TEDC Bandung Polytechnic, Indonesia Dahlan, Informatics Engineering Study Program, TEDC Bandung Polytechnic, Indonesia Dini Rohmayani, Informatics Engineering Study Program, TEDC Bandung Polytechnic, Indonesia

doi> DOI: 10.15575/join.v9i1.1254 Lit Abstract View: 679 № PDF downloads: 509

☑ PDF

Improving with Hybrid Feature Selection in Software Defect Prediction

Muhammad Yoga Adha Pratama, Department of Computer Science, University of Lambung Mangkurat, Kalimantan Selatan, Indonesia

52-60

Rudy Herteno, Department of Computer Science, University of Lambung Mangkurat, Kalimantan Selatan, Indonesia Mohammad Reza Faisal, Department of Computer Science, University of Lambung Mangkurat, Kalimantan Selatan, Indonesia

Radityo Adi Nugroho, Department of Computer Science, University of Lambung Mangkurat, Kalimantan Selatan, Indonesia

Friska Abadi, Department of Computer Science, University of Lambung Mangkurat, Kalimantan Selatan, Indonesia

doi> DOI: 10.15575/join.v9i1.1307 | Abstract View: 646 | PDF downloads: 379

☑ PDF

Water Level Time Series Forecasting Using TCN Study Case in Surabaya

Deni Saepudin, School of Computing, Telkom University, Bandung, Indonesia Egi Shidqi Rabbani, School of Computing, Telkom University, Bandung, Indonesia Dio Navialdy, School of Computing, Telkom University, Bandung, Indonesia Didit Adytia, School of Computing, Telkom University, Bandung, Indonesia

61-69

doi> DOI: 10.15575/join.v9i1.1312 lill Abstract View: 828 № PDF downloads: 433

☑ PDF

Realizing the Promise of Artificial Intelligence in Hepatocellular Carcinoma through Opportunities and **Recommendations for Responsible Translation**

Tamer A. Addissouky, Department of Biochemistry, Science Faculty, Menoufia University, Menoufia; Al-Hadi University College, Baghdad, Iraq; MLS ASCP, United States; MLS Ministry of Health, Alexandria, Egypt https://orcid.org/0000-0003-3797-9155

Majeed M. A. Ali, Al-Hadi University College, Baghdad, Iraq

Ibrahim El Tantawy El Sayed, Department of Biochemistry, Science Faculty, Menoufia University, Menoufia, Egypt Mahmood Hasen Shuhata Alubiady, Al-Hadi University College, Baghdad, Iraq

doi> DOI: 10.15575/join.v9i1.1297 del Abstract View: 813 del PDF downloads: 306

☑ PDF

AI-Powered Real-time Accessibility Enhancement: A Solution for Web Content Accessibility Issues

Samir Dash, Cisco Systems (India) Pvt. Ltd., Bengaluru, Karnataka, India

₿ 80-88

doi > DOI : 10.15575/join.v9i1.1310 Ltd Abstract View : 946 Ltd PDF downloads: 767

☑ PDF

₿ 89-99

Enchancing Lung Disease Classification through K-Means Clustering, Chan-Vese Segmentation, and Canny Edge **Detection on X-Ray Segmented Images**

Joko Riyono, Fakultas Teknologi Industri, Universitas Trisakti, Jakarta, Indonesia Christina Eni Pujiastuti, Fakultas Teknologi Industri, Universitas Trisakti, Jakarta, Indonesia Sofia Debi Puspa, Fakultas Teknologi Industri, Universitas Trisakti, Jakarta, Indonesia Supriyadi, Fakultas Teknologi Industri, Universitas Trisakti, Jakarta, Indonesia Fayza Nayla Riyana Putri, Information System, Universitas Diponegoro, Semarang, Indonesia

PDF

grammarly **1** 29-40



DECLARATION FORM



Declaration Form

MANUSCRIPT TEMPLATE



Manuscript **Template**

JOIN STATS





last update May 27, 2024

https://join.if.uinsgd.ac.id/index.php/join/issue/view/19

Isla Abstract View: 486 I PDF downloads: 496

SAER: Comparison of Rule Prediction Algorithms on Constructing a Corpus for Taxation Related Tweet Aspect-Based Sentiment Analysis

Annisa Mufidah Sopian, 3Department of Informatics, Faculty of Science and Informatics, Universitas Jenderal Achmad 100-110 Yani, Indonesia

Ridwan Ilyas, 3Department of Informatics, Faculty of Science and Informatics, Universitas Jenderal Achmad Yani, Indonesia

Fatan Kasyidi, 3Department of Informatics, Faculty of Science and Informatics, Universitas Jenderal Achmad Yani, Indonesia

Asep Id Hadiana, Faculty of Information and Communication Technology, Universiti Teknikal Malaysia Melaka, Malaysia
Malaysia

 IIII
 Abstract View : 562

 ✓ PDF downloads: 339



Development of a Mobile-Based Application for Classifying Caladium Plants Using the CNN Algorithm

Rudy Chandra, Information Technology, Faculty of Vocational Studies, Institut Teknologi Del, Indonesia https://orcid.org/0000-0002-2267-6365

111-118

Tegar Arifin Prasetyo, Information Technology, Faculty of Vocational Studies, Institut Teknologi Del, Indonesia https://orcid.org/0000-0001-8058-7961

Heni Ernita Lumbangaol, Information Technology, Faculty of Vocational Studies, Institut Teknologi Del, Indonesia Veny Siahaan, Information Technology, Faculty of Vocational Studies, Institut Teknologi Del, Indonesia Johan Immanuel Sianipar, Information Technology, Faculty of Vocational Studies, Institut Teknologi Del, Indonesia

doi > DOI : 10.15575/join.v9i1.1296 [Jul] Abstract View : 508 🗠 PDF downloads: 387



A Mathematical Modelling and Behaviour Simulation of a Smart Grid Cyber-Physical System

Elvis Tamakloe, Department of Computer Engineering, Kwame Nkrumah University of Science and Technology, KNUST- 🖺 119-127 Kumasi, Ghana

Klogo Selorm Griffith, Department of Computer Engineering, Kwame Nkrumah University of Science and Technology, KNUST- Kumasi, Ghana

Benjamin Kommey, Department of Computer Engineering, Kwame Nkrumah University of Science and Technology, KNUST- Kumasi, Ghana

dol > DOI : 10.15575/join.v9i1.1344 | del Abstract View : 409 | ✓ PDF downloads: 226



Performance Comparative Study of Machine Learning Classification Algorithms for Food Insecurity Experience by Households in West Java

Khusnia Nurul Khikmah, IPB University, Indonesia

http://orcid.org/0000-0002-9142-6968

Bagus Sartono, IPB University, Indonesia

Budi Susetyo, IPB University, Indonesia

Gerry Alfa Dito, IPB University, Indonesia

doi> DOI: 10.15575/join.v9i1.1012 | doi | Abstract View: 534 | ✓ PDF downloads: 558



△ PDF

1 128-137

Data Balancing Techniques Using the PCA-KMeans and ADASYN for Possible Stroke Disease Cases

Uung Ungkawa, Department of Informatics, Institut Teknologi Nasional Bandung, Indonesia https://orcid.org/0000-0003-3693-9821

🖺 138-147

Muhammad Avilla Rafi, Department of Informatics, Institut Teknologi Nasional Bandung, Indonesia

doi > DOI: 10.15575/join.v9i1.1293 Lttl Abstract View: 1011 L PDF downloads: 434

△ PDF

Published by:

 $Informatics\ Department,\ Faculty\ of\ Science\ and\ Technology,\ UIN\ Sunan\ Gunung\ Djati\ Bandung.$

Jl. A.H. Nasution No. 105 Cibiru Bandung, Indonesia. 40614. Phone (022) 7800525 / Fax (022) 7803936. Email: join@uinsgd.ac.id p-ISSN: <u>2528-1682</u> e-ISSN: <u>2527-9165</u>



Platform & workflow by OJS / PKP



HOME / Editorial Team

Editorial Team

Editor-in-chief

Dian Sa'adillah Maylawati, Scopus' H-Index: 15, Department of Informatics, UIN Sunan Gunung Djati Bandung, Indonesia

Managing Editor

- Ichsan Budiman, Scopus* H-Index: 2, Department of Informatics, UIN Sunan Gunung Djati Bandung, Indonesia
- Rifqi Syamsul Fuadi, Scopus H-Index: 3, UIN Sunan Gunung Djati Bandung, Indonesia

Editorial Board

- 1. Asif Ali Laghari, Scopus H-Index: 26, Sindh Madressatul Islam University, Pakistan.
- 2. Muhammed Ali Abdul Hameed, Scopus' H-Index: 16, Fuel Cell Institute Universiti Kebangsaan Malaysia, Malaysia.
- 3. Anton Abdulbasah Kamil, Scopus H-Index: 15, Nisantasi University, Turkey.
- Saiyed Umer, Scopus* H-Index: 16, Department of Computer Science & Engineering Aliah University, Newtown, Kolkata-700156. India.
- 5. <u>Vadim A. Zhmud</u>, Scopus* H-Index: 12, Novosibirsk Institute of Software Systems, Russia.
- 6. <u>Wildan Budiawan Zulfikar</u>, Scopus H-Index: 10, UIN Sunan Gunung Djati Bandung, Indonesia.
- 7. Ali Rahman, Scopus* H-Index: 5, UIN Sunan Gunung Djati Bandung, Indonesia.
- 8. <u>Ichsan Taufik</u>, Scopus H-Index: 5, PhD Student in Asia e-University, Malaysia.
- 9. Rio Guntur Utomo, Scopus H-Index: 5, University of Southampton, United Kingdom.
- 10. Yazan Abdelmajid Abu Huson, Scopus' H-Index: 4, Department of Accounting, University of Valencia, Spain.
- 11. Vedapradha R, Scopus' H-Index: 3, School of Commerce Mount Carmel College, Autonomous, India.
- 12. Rian Andrian, Scopus* H-Index: 3, Universitas Pendidikan Indonesia, Indonesia.
- 13. Nur Lukman, Scopus H-Index: 2, PhD Student in Asia e-University, Malaysia.
- 14. Shavkat Seytov, Scopus H-Index: 2, Tashkent State University of Economics, Uzbekistan.
- Dina Hamdy Darwish, Scopus* H-Index: 2, Department of Artificial Intelligence, Faculty of Computer Science and Information Technology, Ahram Canadian University, Egypt.

Editor Advisory Board

- 1. Muhammad Ali Ramdhani, Scopus H-Index: 25, UIN Sunan Gunung Djati Bandung, Indonesia
- 2. Giacomo Cabri, Scopus* H-Index: 23, Department FIM, University of Modena and Reggio Emilia, Italy.
- 3. Anjar Wanto, Scopus H-Index: 16, STIKOM Tunas Bangsa Pematangsiantar, Indonesia.
- 4. Tanweer Alam, Scopus* H-Index: 16, Islamic University of Madinah, Saudi Arabia.
- 5. Ayu Purwarianti, Scopus* H-Index: 15, Institut Teknologi Bandung, Indonesia.
- 6. <u>A'ang Subiyakto</u>, Scopus H-Index: 13, UIN Syarif Hidayatullah Jakarta, Indonesia.
- 7. Rinaldi Munir, Scopus H-Index: 10, Institut Teknologi Bandung, Indonesia.
- 8. Husni Teja Sukmana, Scopus H-Index: 10, UIN Syarif Hidayatullah Jakarta, Indonesia.
- 9. Mohamad Irfan, Scopus H-Index: 9, Asia e-University, Malaysia.
- 10. Mailasan Jayakrishnan, Scopus H-Index: 8, Xiamen University Malaysia, Malaysia.
- 11. Moch Arif Bijaksana, Scopus H-Index: 8, Telkom University, Indonesia.
- 12. <u>Satrya Fajri Pratama</u>, Scopus* H-Index: 7, Sheffield Hallam University, Sheffield, **United Kingdom.**

MAKE A SUBMISSION

ACCREDITED



EDITORIAL TEAM

CITEDNESS IN SCOPUS

PEER REVIEW PROCESS

FOCUS AND SCOPE

PUBLICATION ETHICS

AUTHOR GUIDELINES

AUTHOR FEES

DATA SHARING POLICY

REVENUE SOURCES

ADVERTISING POLICY

DIRECT MARKETING

RETRACTION-CORRECTIONS

COPYRIGHT NOTICE

PLAGIARISM CHECK

REFERENCES MANAGEMENT

JOURNAL HISTORY

TOOLS



- 13. Yana Aditia Gerhana, Scopus' H-Index: 7, Asia e-University, Malaysia.
- 14. Wisnu Uriawan, Scopus H-Index: 6, University of Lyon (INSA de Lyon), France.
- 15. Ahmad Wisnu Mulyadi, Scopus' H-Index: 5, Virtual Patient Engine, Artificial Intelligence Research Team, BioMed X, Germany.
- Ahmad Ashraf Abdul Halim, Scopus' H-Index: 5, Faculty of Electronic Engineering & Technology (FKTEN), Universiti Malaysia Perlis (UniMAP), Malaysia.
- 17. Cecep Nurul Alam, Scopus' H-Index: 5, Asia e-University, Malaysia.
- 18. Ana Hadiana, Scopus* H-Index: 5, Research Center for Informatics, BRIN, Indonesia.
- 19. Esa Firmansyah, Scopus' H-Index: 5, STMIK Sumedang, Indonesia.
- 20. <u>Vandha Pradwiyasma Widartha</u>, Scopus' H-Index: 4, Department of Information System, Pukyong National University, South Korea.
- 21. Santosh Gore, Scopus' H-Index: 4, Director, Sai Info Solution, India.
- 22. <u>Aulia Akhrian Syahidi</u>, **Scopus*** H-Index: 4, Smart City Information System Study Program, Politeknik Negeri Banjarmasin, **Indonesia**.
- 23. Setio Basuki, Scopus H-Index: 4, Universitas Muhammadiyah Malang, Indonesia.
- 24. Arini Arini, Scopus H-Index: 4, UIN Syarif Hidayatullah Jakarta, Indonesia.
- 25. Muhammad Irwan Padli Nasution, Scopus' H-Index: 4, UIN Sumatera Utara, Indonesia.
- 26. Nunik Destria Arianti, Scopus H-Index: 4, Universitas Nusaputra, Indonesia.
- 27. <u>Dian Nuraiman</u>, Scopus H-Index: 3, RMIT University, Australia, Australia.
- Abdelaaziz Hessane, Scopus H-Index: 3, Department of Computer Sciences, FSTE, Moulay Ismail University of Meknès, Morocco.
- 29. <u>Undang Syaripudin</u>, Scopus H-Index: 3, Asia e-University, Malaysia.
- 30. Mohamed Osman Suliman Omara, Scopus' H-Index: 2, International College of Semiconductor Technology National Yang Ming Chiao Tung University, Taiwan.
- 31. Chan Voeun, Scopus' H-Index: 1, National Polytechnic Institute of Cambodia, Cambodia.
- 32. Areeg Alfouri, Scopus' H-Index: 1, Faculty of Medicine Al-Balqa Applied University, Jordan.
- 33. <u>G Vinoda Reddy</u>, Scopus' H-Index: 1, Department CSE(Al&ML), CMR Technical Campus, Medichal Hyderabad, India.

English Language Advisor

Kiki Nuriska Denhas, Scopus* H-Index: 1, Universitas Islam Negeri Walisongo Semarang, Indonesia





DECLARATION FORM



Declaration Form

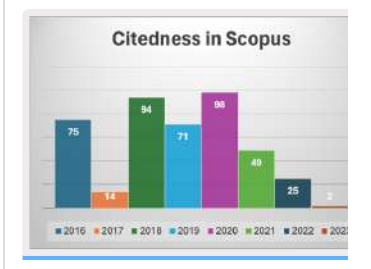
MANUSCRIPT TEMPLATE



Manuscript Template

JOIN STATS





last update May 27, 2024

Published by:

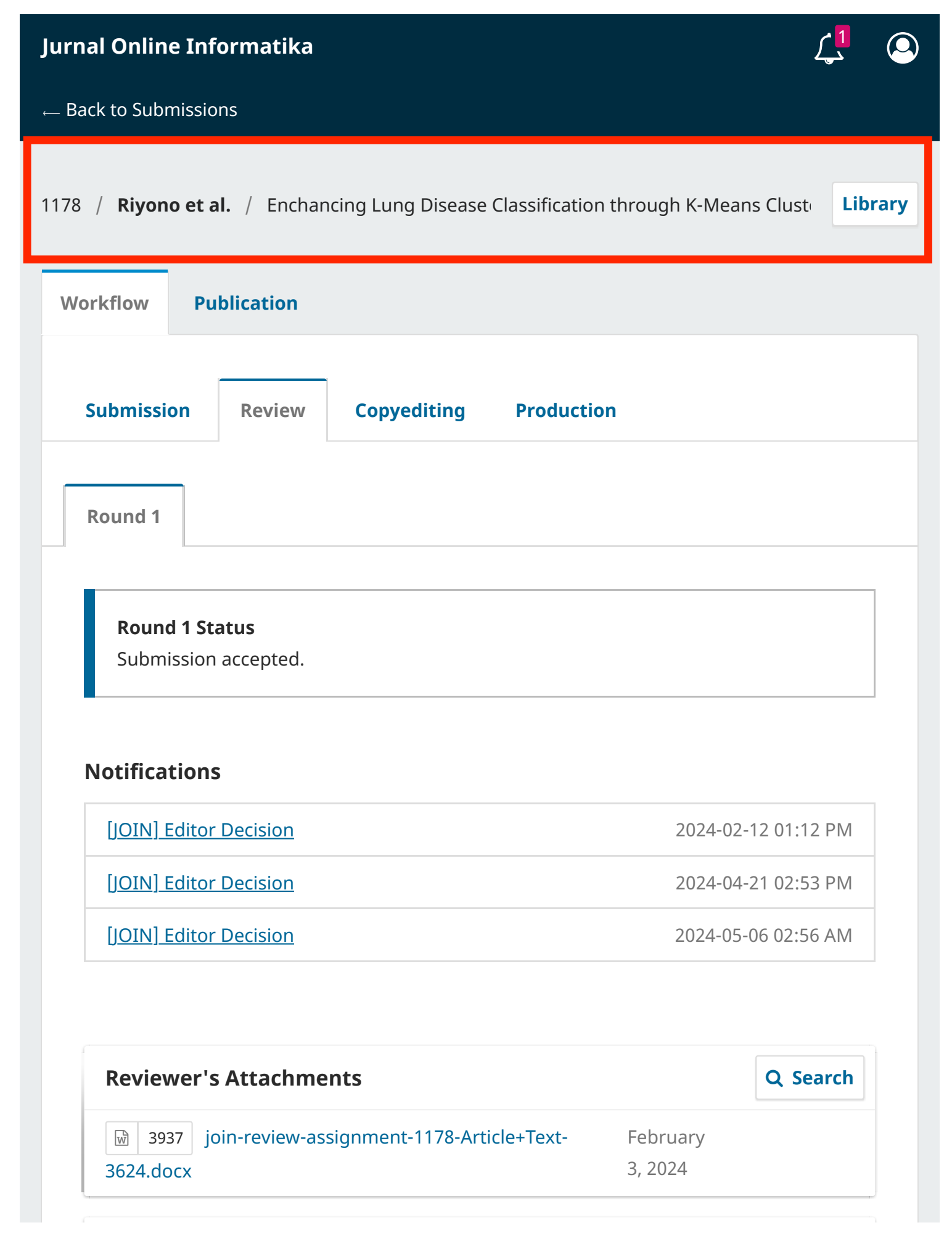
Informatics Department, Faculty of Science and Technology, UIN Sunan Gunung Djati Bandung.

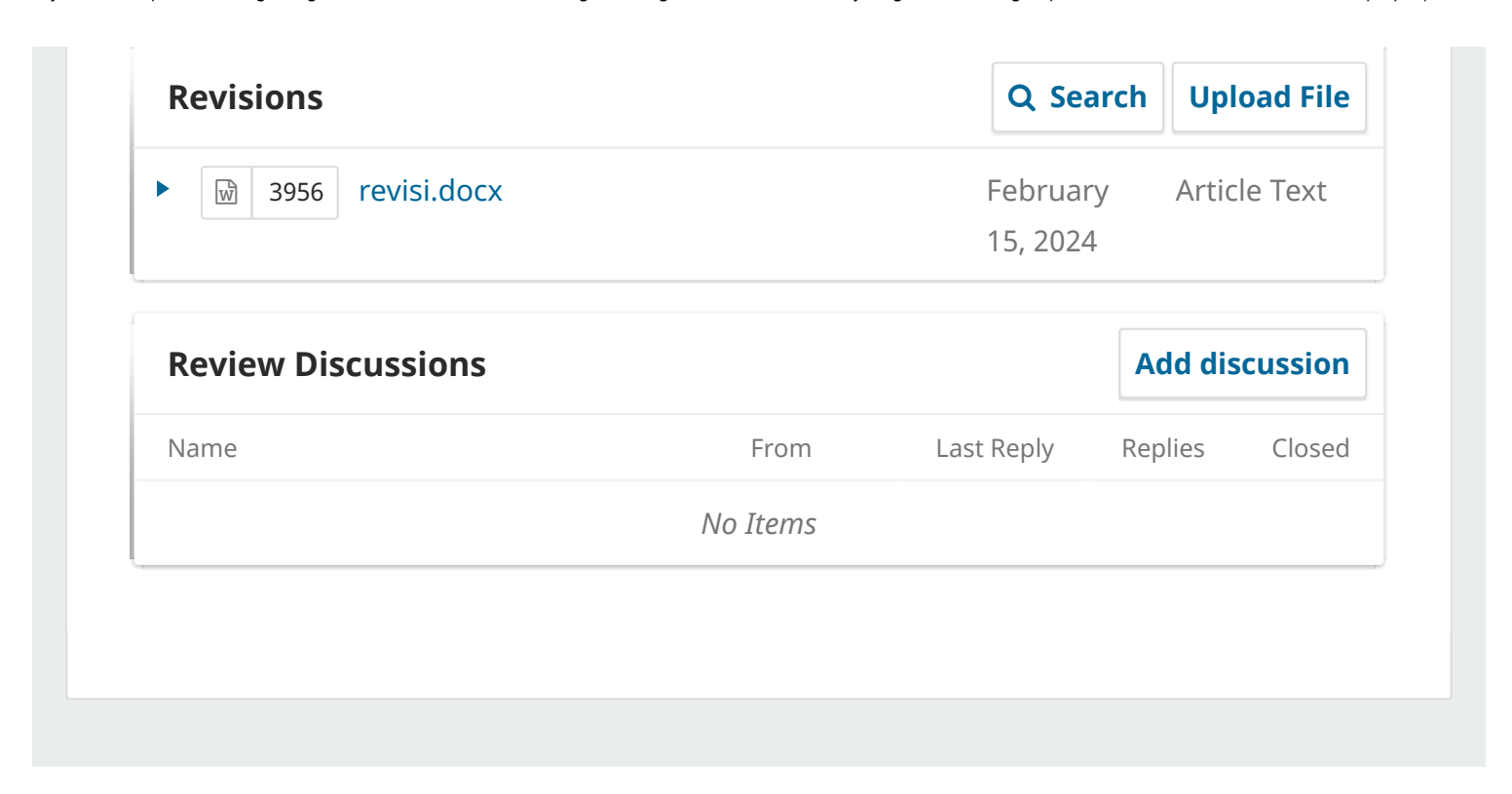
Jl. A.H. Nasution No. 105 Cibiru Bandung, Indonesia. 40614. Phone (022) 7800525 / Fax (022) 7803936. Email: join@uinsgd.ac.id p-ISSN: 2528-1682 e-ISSN: 2527-9165



 $This work is \ licensed \ under \ a \ \underline{Creative\ Commons\ Attribution-NoDerivs\ 2.0\ Generic\ License}.$

Platform & workflow by OJS / PKP







JOIN (Jurnal Online Informatika)

p-ISSN: 2528-1682, e-ISSN: 2527-9165 Volume 9 Number 1 | June 2024: 89-99

DOI: 10.15575/join.v9i1.1178

Enchancing Lung Disease Classification through K-Means Clustering, Chan-Vese Segmentation, and Canny Edge Detection on X-Ray Segmented Images

Joko Riyono¹, Christina Eni Pujiastuti², Sofia Debi Puspa³, Supriyadi⁴, Fayza Nayla Riyana Putri⁵

1,2,3,4</sup>Fakultas Teknologi Industri, Universitas Trisakti, Jakarta

5Information System, Universitas Diponegoro, Semarang

Article Info

Article history:

Received September 02, 2023 Revised February 15, 2024 Accepted April 21, 2024 Available Online May 06, 2024

Keywords:

Canny Chan-Vese K-Means Clustering Lungs Segmentation X-Ray Image

ABSTRACT

The lungs are one of the vital organs in the human body. Not only play a role in the respiratory system, the lungs are also responsible for the human circulatory system. Supporting examinations can also facilitate medical workers in determining the diagnosis. Usually a lung examination is complemented by a chest X-ray examination procedure. This examination aims to see directly and assess the severity of lung conditions. With current technological advances, image analysis can be done easily. Through digital image processing methods, information can be obtained from images that can be used for analysis as a support for diagnoses in the world of health. Image segmentation is a method in which digital images are divided into several segments or subgroups based on the characteristics of the pixels in the image. In this study, clustering with the K-Means method will be carried out on the results of segmentation of x-ray images of lung diseases, namely Covid-19, Tuberculosis, and Pneumonia. The segmentation method that will be implemented is the Chan-Vese Method and the Canny Edge Detection Method. This research shows that the results of the accuracy of applying the K-Means Clustering method to Chan-Vese and Canny Edge-Based Image Segmentation are 80%.

Corresponding Author:

Joko Riyono,

Fakultas Teknologi Industri, Universitas Trisakti, Jakarta, Indonesia.

Email: jokoriyono@trisakti.ac.id

1. INTRODUCTION

The lungs are one of the vital organs in the human body. Not only play a role in the respiratory system, the lungs are also responsible for the human circulatory system. Lung health can be influenced by many factors such as lifestyle, environmental hygiene, and heredity [1]. If there is a malfunction in the lungs, human health will be disrupted as a whole. Therefore, examination of lung malfunction should be done as early as possible.

The procedure carried out in a lung examination usually requires investigations because lung diseases generally have similar symptoms such as coughing, fever, decreased body weight, loss of appetite, and so on [2]. Supporting examinations can also facilitate medical workers in determining the diagnosis. Usually a lung examination is complemented by a chest X-ray examination procedure [3]. This examination aims to see directly and assess the severity of lung conditions.

The chest X-ray procedure provides an image based on the diffraction of electromagnetic waves, namely X-rays. The use of this light makes it possible to see human organs visually without having to do a surgical procedure (non-invasive procedure). This procedure produces a two-dimensional image as a representation of the condition of the lungs in the human body and basically this examination is only done through visual observation [4]. Therefore, of course, proper analysis is needed in determining the diagnosis through chest X-ray images.

p-ISSN: 2528-1682 e-ISSN: 2527-9165

With current technological advances, image analysis can be done easily. Through digital image processing methods, information can be obtained from images that can be used for analysis as a support for diagnoses in the world of health. Of course, this can also be applied to chest x-ray images.

Digital image processing is one of the areas of research in computer science. Broadly speaking, digital image processing works by analyzing digital images in such a way as to obtain a more perfect image. Not only that, image processing in research is also used in extracting information on images as needed. To extract information on several parts of an image, it is usually done with the segmentation method first.

Basically, the segmentation method is used to separate objects in an image. Image segmentation works by dividing digital images into several segments based on the characteristics of the image. This method allows for the separation of objects from the background. This is of course very necessary in research related to image analysis to extract or obtain information from the desired parts of the image.

Image segmentation is a method in which digital images are divided into several segments or subgroups based on the characteristics of the pixels in the image [5]. This aims to reduce the detector's inference time when processing the entire image because with segmentation, the detector does not need to process the entire image but only the region selected by the segmentation algorithm. Image segmentation aims to classify areas that have similarities so that they can also distinguish objects in the image from their background [6].

There are two segmentation techniques that are often used and can be divided into two categories, namely Region Segmentation which is a segmentation technique to find regions that meet certain homogeneity criteria such as finding color values that have similarities with other pixels so that they can be used as one region and Edge-Based Segmentation which is a technique for finding edges between regions between different characteristics [7].

The Chan-Vese strategy could be a locale division procedure, which could be a strategy that works without borders. The dynamic form show is one of the working models of division procedure that employments vitality and constrain imperatives on the picture into cluster locales [6]. The dynamic form demonstrate is commonly utilized in different picture preparing applications, particularly in therapeutic picture processing such as chest X-ray pictures, brain CT looks or MRI pictures of organs. Positive edge models are utilized in advanced picture preparing by pixel separation. The Chan-Vese strategy is utilized to distinguish visual objects with developmental energies. The advancement of the Mumford-Shah demonstrate and this demonstrate is based on the vitality diminishment issue, which can be reexpressed as equations of unequivocal levels, driving to a less difficult way of understanding the issue [8].

Canny identify is an edge-based division method found by John F.Canny in 1986 [9]. Basically, the Canny strategy works by employing a grayscale picture as input and producing concentrated discontinuities as yield or edge images. In its application, there are steps for shrewd edge location strategy i.e. smooth or channel commotion, calculate incline quality or slope course, apply delay edge prepare setting, not max [10]. This strategy has criteria that moreover ended up its advantage in picture division strategy, specifically Canny Detector has the capacity to distinguish edges based on indicated convolution parameters and is adaptable in decide the level of edge thickness discovery, to supply a least of separate between the edge of the location result and the initial edge, as it were one reaction on each edge to play down clutter within the post-processing step there [11].

Previous research has been carried out by Elsha Heny Pratiwi and Dwi Juniandi in 2022 regarding their research entitled Clustering Lung Disease Based on Chest X-Rays Using Fractal Dimensions Box Counting and K-Medoids. In his research, clustering of lung diseases was carried out based on the results of information from x-ray images of the lungs obtained through the canny segmentation method and resulted in an accuracy of 87% [12].

In this study, clustering with the K-Means method will be carried out on the results of segmentation of x-ray images of lung diseases, namely Covid-19, Tuberculosis, and Pneumonia. The segmentation method that will be implemented is the Chan-Vese Method and the Canny Edge Detection Method.

2. METHOD

This research was conducted through a quantitative approach because the entire process was carried out using data in the form of numbers as an analytical tool. The data in this research is a type of data in the form of images obtained from previous studies. It can be said, the data used in this study is secondary data. Secondary data is data that is already available and collected by other parties outside the agency under study. Secondary data can generally be obtained through websites, books, articles,

internal organizational records and so on [13]. In this study, data was obtained through a site that contains many types of datasets that are commonly used by researchers in conducting research, namely Kaggle.

The image data used as the research subject is an x-ray image of the chest from patients with Covid-19 lung disease, tuberculosis, pneumonia, and healthy lungs which will also be used to extract information from the image in the form of numerical data from the results of segmentated image. This numeric data will be used again in the clustering process to produce disease cluster classes based on the number of white pixel areas in the segmented image. In this study, there are several stages described as a flowchart as shown in Figure 1 below:

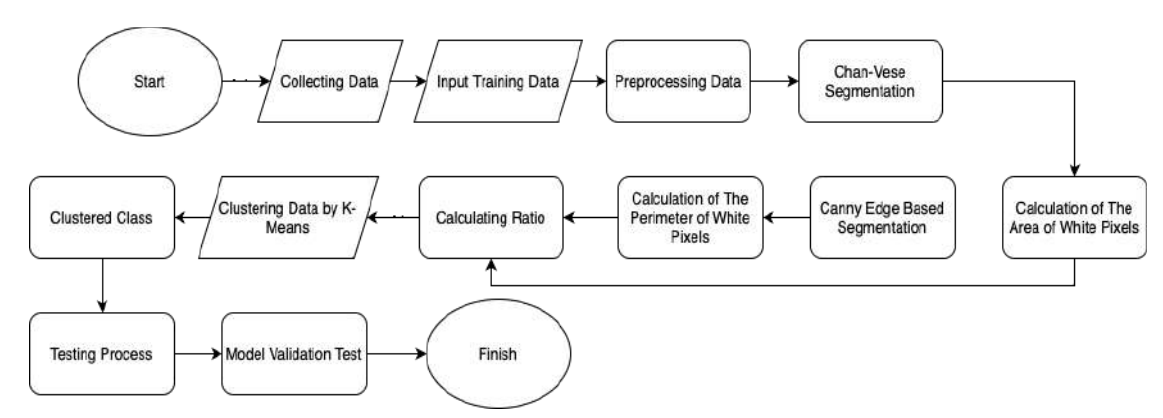


Figure 1. Research Methods Flowchart

The segmentation process applied to the image aims to obtain the features used in the analysis process, in this case, namely the white area in the segmented image [14]. This white area represents the damaged area of the lungs. Before the segmentation process is carried out, the image goes through several two stages in the data preprocessing process, namely the Resize process, Grayscaling Process and the Filtering process with Histogram Equalization.

The image segmentation process is carried out twice, namely by the Chan-Vese method and Canny edge detection. The Chan-Vese method is an improvement from the edge-based model, because it bases edge detection on an image not based on image gradients but is based on curve evolution techniques, the Mumford-shah function for segmentation and level set [6]. This is because, detection using image gradients is less effective because discrete gradients are limited and the stop function is never null at an edge and allows the curve to pass through the existing boundaries. In the Chan-Vese model, initial contours can be applied anywhere in the image and the Chan-Vese model will automatically detect all contours, regardless of the position of the original contours. Active contour models are commonly used in various image processing applications, especially in medical image processing, such as chest X-ray images, brain CT scans or MRI images of the body. Positive edge models are used in digital image processing through pixel separation. The evolution of the Mumford-Shah model and this model is based on the energy reduction problem, which can be reformatted in the formula of definite levels, making the problem easier to solve [6].

Edge detection in an image is a process that produces the edges of an image object, its purpose is to mark the part that becomes a detailed image. Canny edge detection is one of the edge detection algorithms that has a minimum error rate and produces optimal edge images [15]. The edge (edge) is a sudden (large) change in the value of the intensity of gray degrees in a short distance. The purpose of edge detection is to group objects in the image, and is also used to further analyze the image.

The segmentation process, crucial for feature extraction, employed two methods: Chan-Vese and Canny edge detection. The Chan-Vese method, based on curve evolution techniques and Mumford-Shah function, aimed to detect damaged areas in the lungs by focusing on the white regions in segmented images. The Canny edge detection, known for its minimum error rate and optimal edge images, identified sudden changes in intensity, marking detailed parts of the images. Both methods contributed to obtaining precise data on the white pixel area representing lung damage

After the segmentation process is complete, numerical data will be obtained in the form of white pixel area in the image which will then be used in the clustering process to group the data into several classes, namely the Covid-19 class, Tuberculosis, Pneumonia, and Normal or healthy lung class. Mathematically, K-Means clustering is carried out in 4 stages as [16]:

1. Initialize the centroid values randomly

 $v = \frac{\sum_{i-1}^{n} \chi_i}{n}; = 1, 2, 3, ... n$ (1)

Information:

v: centroid on cluster

x_i: i-th object

n: number of objects/number of cluster member objects.

2. Place each data point to the nearest centroid by calculating the distance of each data point to the centroid in Euclidean distance

$$(x,y) = ||x-y|| = \sqrt{\sum_{i=1}^{n} (x_i - y_i)^2}, i = 1,2,3,...n$$
 (2)

Information: xi:ith x object yi:y-th power

n: number of objects

- 3. Recalculate the centroid of the newly formed cluster by calculating the mean of each data point in the cluster.
- 4. Perform optimization to meet the criteria by repeating the last two steps.

The research strategy systematically applied these methods, and testing procedures involved applying the segmentation methods to chest X-ray images, extracting numerical data, and using K-Means clustering to classify diseases and healthy lungs based on the white pixel area in the segmented image. The research incorporated a robust testing process to evaluate the effectiveness of the applied methodologies. Each dataset was labeled with respective class names, facilitating the testing process. The assessment involved comparing the number of white pixels in test images to predetermined clustering classes.

3. RESULT AND DISCUSSION

The first stage in this study was to collect x-ray image data used as objects in this study. Data in the form of digital data will be processed in the Joint Photographic Experts Group (*jpeg) format. The x-ray image data used is x-ray data including Covid-19 disease, Tuberculosis, Pneumonia and healthy lungs.

Table 1. Datasets

No.	Class	Total Data
1	Covid-19	107
2	Tuberculosis	651
3	Pneumonia	752
4	Normal Lungs	1342

In table 1, there are types and amounts of data used in this research process. All data is collected through the Kaggle website which provides various kinds of datasets for research purposes. This data is obtained by downloading the required dataset.

The next step is image preprocessing. The image epreprocessing stage goes through three stages which aim to improve the quality of the raw data (image) before further analysis. These three stages are resizing all image sizes to 256x256 pixels so that all images are the same size, changing all RGB images to Grayscaling images, and carrying out the filtering process with the Histogram Equalization Method.

3.1. Preprocessing Process

3.1.1. Image Resizing Process

The normalization process in the image aims to change the size of the image resolution so that all images have the same resolution size. Changes in the size of the image resolution will be equated to 256×256 pixels. With a size of 256×256 pixels, the image size can be represented as a matrix with 256 rows and 256 columns. Image size normalization process is done by imresize function via MATLAB. This process will display an image with a size of 256×256 as shown below:

p-ISSN: 2528-1682 e-ISSN: 2527-9165

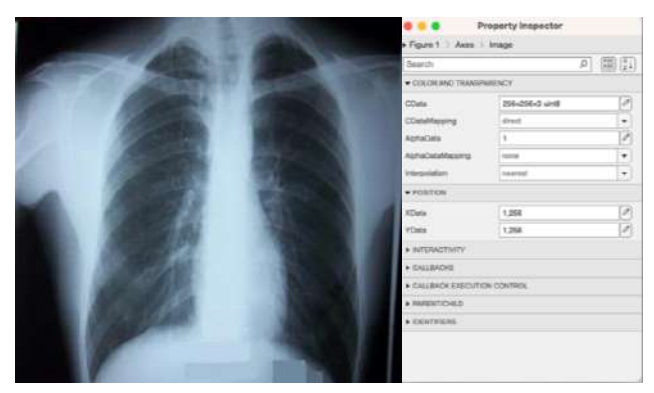


Figure 2. Resize Image

3.1.2. Grayscalling Image Process

The grayscaling process in the image aims to change the RGB (Red, Green, Blue) image to a grayscale image with an intensity of 0 to 255 (8-bit image). The grayscalling process in MATLAB is done with the function rgb2gray. The results of this stage can be seen in the Figure 3 below:



Figure 3. Grayscalling Image

3.1.3. Filtering Image Process With Histogram Equalization

Filtering process aims to improve image quality by reducing noise and adjusting image brightness. The filtering process in this research uses the Histogram Equalization method, which is a graphic equalization that represents the distribution of grayscale image intensities [19]. The filtering process in this study uses the Histogram Equalization technique, which is a graphic equalization process that represents the distribution of grayscale image intensities [17]. This process is done with the histeq function in MATLAB. The image on the right from Figure 5 shows that the image already has better contrast and a flatter histogram than Figure 4.

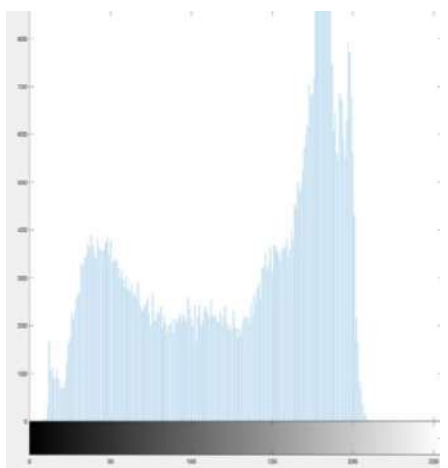


Figure 4. Before Filtering

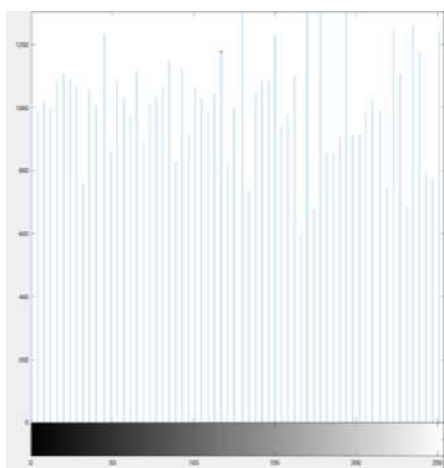


Figure 1. After Filtering

p-ISSN: 2528-1682 e-ISSN: 2527-9165

3.2. Calculation Process of The White Area of The Chan-vese Segmentation Image

The normalization process in the image aims to change the size of the image resolution so that all images have the same resolution size. Changes in the size of the image resolution will be equated to 256×256 pixels. With a size of 256×256 pixels, the image size can be represented as a matrix with 256 rows and 256 columns [18]. Image size normalization process is done by imresize function via MATLAB. This process will display an image with a size of 256×256 as shown below:

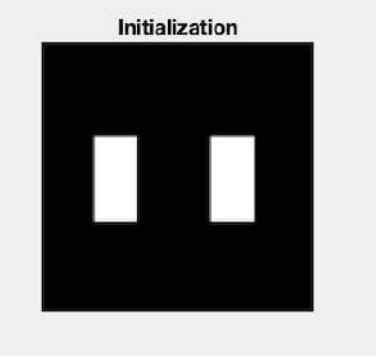


Figure 6. Initialization Mask

The segmentation process using the Chan-Vese method will produce black and white images as shown in Figure 7 which is a comparison of the images before and after segmentation.

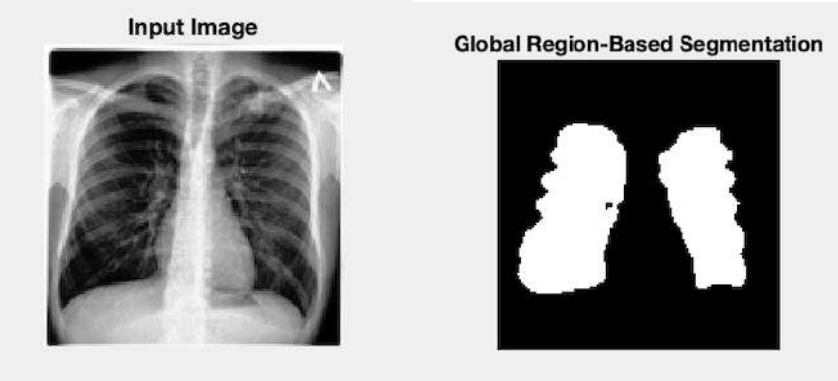


Figure 7. Comparison of Raw and Segmented Image

The next step is to convert the segmented image into a binary image with the im2bw function and fill in imperfect image areas that have holes with the imfill function. After everything has been done, the calculation of the area of white pixels in the image can be done with the regionprops function, which is a function in Matlab that is used to measure the properties of a binary image. Data on the area of white pixels in segmented images can be seen in Table 2 for Covid-19, Table 3 for Tuberculosis, Table 4 for Pneumonia, Table 5 for Normal Lungs.

Table 2. Area of White Pixels of Covid-19 Image

No.	Data	Area	
1	'COVID19(460) Small.jpeg'	2060	
2	'COVID19(461) Small.jpeg'	2070	
3	'COVID19(462) Small.jpeg'	2313	
4	'COVID19(463) Small.jpeg'	2416	
5	'COVID19(464) Small.jpeg'	3384	

Table 3. Area of White Pixels of Tuberculosis Image

No.	Data	Area
1	'Tuberculosis-1 Small.jpeg'	4326
2	'Tuberculosis-10 Small.jpeg'	3676
3	"Tuberculosis-100 Small.jpeg"	4255
4	"Tuberculosis-101 Small.jpeg"	4462
5	'Tuberculosis-102 Small.jpeg'	3340

Table 4.	Area of Wh	ite Pixels	of Pneum	onia Image

		O .	
No.	Data	Area	
1	'person1000_2931.jpeg'	3320	
2	'person1000_1681.jpeg'	2040	
3	'person1000_2932.jpeg'	1799	
4	'person1000_2932.jpeg'	1761	
5	'person1000_2934.jpeg'	3039	
	Table 5. Area of White Pixels of No	rmal Lungs Image	
No.	Data	Area	
1	'IM-0115-0001.jpeg'	2194	
2	'IM-0117-0001.jpeg'	1842	
3	'IM-0119-0001.jpeg'	1732	
4	'IM-0122-0001.jpeg'	2010	
5	'IM-0125-0001.ineg'	1787	

3.3. Calculation Process of The White Area of The Canny Edge-Based Segmentation Image

The next image segmentation process uses the second method, namely Canny Edge Detection. With this process, we will find a border around the chan-vese segmented image by detecting changes in brightness levels and generating the circumference of the image as another variable needed in the clustering process.

This segmentation process uses the edge function in Matlab. By using the edge function, an image of the Canny edge detection results will be obtained as shown in Figure 9 below.

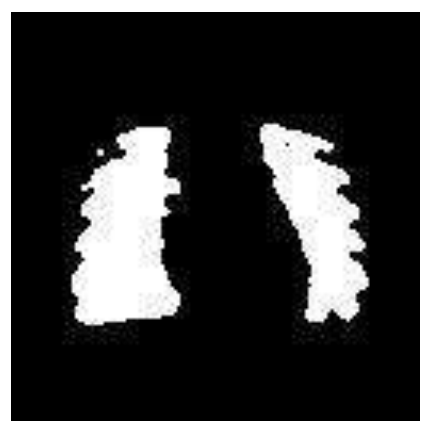


Figure 8. Chan-Vese Segmentation

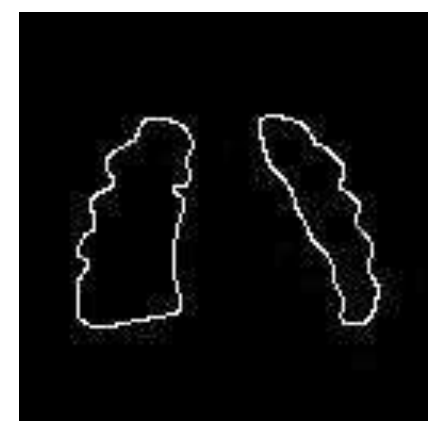


Figure 9. Canny Segmentation

Through the image segmentation results from Chan-Vese and then Canny, we get the circumference of the edge that surrounds the image. The results are described in the Table 6 for Covid-19, Table 7 for Tuberculosis, Table 8 for Pneumonia, Table 9 for Normal Lungs.

Table 6. White Pixels Circumference of Covid-19 Image

		· ·
No.	Data	Circumference
1	'COVID19(460) Small.jpeg'	499
2	'COVID19(461) Small.jpeg'	401
3	'COVID19(462) Small.jpeg'	376
4	'COVID19(463) Small.jpeg'	431
5	'COVID19(464) Small.jpeg'	446

Table 7. White Pixels Circumference of Tuberculosis Image

		-
No.	Data	Circumference
1	'Tuberculosis-1 Small.jpeg'	484
2	"Tuberculosis-10 Small.jpeg"	480
3	'Tuberculosis-100 Small.jpeg'	474
4	'Tuberculosis-101 Small.jpeg'	492
5	'Tuberculosis-102 Small.jpeg'	479

p-ISSN: 2528-1682 e-ISSN: 2527-9165

Table 8. White Pixels Circumference of Pneumonia Image

No.	Data	Circumference
1	'person1000_2931.jpeg'	586
2	'person1000_1681.jpeg'	382
3	'person1000_2932.jpeg'	394
4	'person1000_2932.jpeg'	399
5	'person1000_2934.jpeg'	346

Table 9. White Pixels Circumference of Normal Lungs Image

No.	Data	Circumference
1	'IM-0115-0001.jpeg'	491
2	'IM-0117-0001.jpeg'	498
3	'IM-0119-0001.jpeg'	468
4	'IM-0122-0001.jpeg'	397
5	'IM-0125-0001.jpeg'	491

3.4. Calculating Ratio

So far, area and circumference data have been obtained from the segmented image. Furthermore, ratio calculations are carried out because the size of human lungs has different sizes. With this step, the data can be used for the next clustering process.

This process is done by the equation (3). For example, one of the data calculations for the Covid-19 data below:

- Number of White Pixel (Canny Edge-Based Segmentation) of "COVID19(460) Small.jpeg": 491
- Number of White Pixel (Chan-Vese Segmentation) of "COVID19(460) Small.jpeg": 2060

Calculation:
$$\frac{\text{The Number of Pixels of The Canny Detection Segmented Image}}{\text{The Number of Pixels of The Chan-Vese Segmented Image}} = \frac{491}{2060} = 4,12825651$$
 (3)

From the calculation results above, it can be concluded that the number of white pixels in the "COVID19(460) Small.jpeg" image is 4.12825651. The same process applies to all images and the results are as shown in the table below, The research involved a detailed analysis of various medical images, and the results are presented in Tables 10 to 13, showcasing the white pixel ratios for different categories of lung images. Each table provides specific details for the examined images, including the file names, circumference, area, and the calculated white pixel ratio.

Table 10. White Pixels Ratio of Covid-19 Image

	-				
No	o. Data	Circumference	Area	Ratio	
1	'COVID19(460) Small.jpeg'	499	2060	0,24223301	
2	'COVID19(461) Small.jpeg'	401	2070	0,19371981	
3	'COVID19(462) Small.jpeg'	376	2313	0,16255945	
4	'COVID19(463) Small.jpeg'	431	2416	0,17839404	
5	'COVID19(464) Small.jpeg'	446	3384	0,13179669	

Table 10 outlines the white pixel ratios for several Covid-19 chest X-ray images. Each entry includes the file name, circumference, area, and the calculated ratio. For instance, 'COVID19(460) Small.jpeg' has a circumference of 499, an area of 2060, and a calculated ratio of 0.24223301

Table 11. White Pixels Ratio of Tuberculosis Image

No.	Data	Circumference	Area	Ratio
1	"Tuberculosis-1 Small.jpeg"	484	4326	0,11188165
2	'Tuberculosis-10 Small.jpeg'	480	3676	0,19371981
3	'Tuberculosis-100 Small.jpeg'	474	4255	0,16255945
4	'Tuberculosis-101 Small.jpeg'	492	4462	0,17839404
5	'Tuberculosis-102 Small.jpeg'	479	3340	0,13179669

In Table 11, the white pixel ratios for Tuberculosis chest X-ray images are presented. Similar to Table 10, it includes file names, circumference, area, and the calculated ratio. For example, 'Tuberculosis-1 Small.jpeg' has a circumference of 484, an area of 4326, and a calculated ratio of 0.11188165.

Table 12. White Pixels Ratio of Pneumonia Image

No.	Data	Circumference	Area	Ratio
1	'person1000_2931.jpeg'	586	3320	0,17650602
2	'person1000_1681.jpeg'	382	2040	0,19371981
3	'person1000_2932.jpeg'	394	1799	0,16255945
4	'person1000_2932.jpeg'	399	1761	0,17839404
5	'person1000_2934.jpeg'	346	3039	0,13179669

Table 12 provides information on the white pixel ratios for Pneumonia chest X-ray images. Each entry includes the file name, circumference, area, and the calculated ratio. 'person1000_2931.jpeg' has a circumference of 586, an area of 3320, and a calculated ratio of 0.17650602, as an example

Table 13. White Pixels Ratio of Normal Lungs Image

			_	_	
No.	Data	Circumference	Area	Ratio	
1	'IM-0115-0001.jpeg'	491	2194	0,22379216	
2	'IM-0117-0001.jpeg'	498	1842	0,27035831	
3	'IM-0119-0001.jpeg'	468	1732	0,27020785	
4	'IM-0122-0001.jpeg'	397	2010	0,19751244	
5	'IM-0125-0001.jpeg'	491	1787	0,27476217	

The white pixel ratios for images of normal lungs are detailed in this table. It includes file names, circumference, area, and the calculated ratio. 'IM-0115-0001.jpeg' has a circumference of 491, an area of 2194, and a calculated ratio of 0.22379216, as one example. These tables collectively provide a comprehensive overview of the white pixel ratios across different types of chest X-ray images, contributing valuable insights into the characteristics of each category.

3.5. Clustering Data by K-Means

After all image processing has been completed, the next step is the clustering process using the K-Means method. This process begins by calculating the average of all data including data on the ratio of Covid-19, Tuberculosis, Pneumonia, and Healthy Lungs. The average value is obtained with the data from the previous ratio calculation process.

Table 14. Mean Value Data

No.	Data	Average (Mean)
1	Covid-19 Lungs	0.16540681
2	Tuberculosis Lungs	0.10936217
3	Pneumonia Lungs	0.2004141
4	Normal Lungs	0.24035373

As in the table 14, you can see the average of each disease data. This clustering process is carried out so that four cluster classes are obtained, namely Cluster 0, Cluster 1, Cluster 2, Cluster 3. Determining the name of the cluster is done by finding the value that is closest to the average in the data for each disease. Cluster 0 has the closest value to the average value in the Covid-19 data, as well as Cluster 1 for Tuberculosis data, Cluster 2 for Pneumonia data, Cluster 3 for Normal Lung data. The clustering process is carried out using the Jupyter Notebook software and the cluster results and centroid values are shown in the table below:

 $Table\ 15.\ Centroid\ for\ Each\ Cluster$

No.	Cluster	Centroid
1	Cluster 0 (Covid-19 Lungs)	0.154021
2	Cluster 1 (Tuberculosis Lungs)	0.083526
3	Cluster 2 (Pneumonia Lungs)	0.189932
4	Cluster 3 (Normal Lungs)	0.239203

The clustering process was executed using the Jupyter Notebook software, a popular tool for interactive and collaborative data analysis. The results of this process, including the identified clusters and their corresponding centroid values, are summarized in Table 15. This table elucidates the outcomes of the clustering process, showcasing the centroids for each identified cluster. The clusters are differentiated based on the types of lung conditions:

- 1. Cluster 0 (Covid-19 Lungs): The centroid value for this cluster is 0.154021, representing the average position of data points within the cluster. This centroid is indicative of the characteristics associated with chest X-ray images depicting Covid-19 affected lungs.
- 2. Cluster 1 (Tuberculosis Lungs): With a centroid value of 0.083526, this cluster represents the average features of chest X-ray images illustrating Tuberculosis affected lungs.
- 3. Cluster 2 (Pneumonia Lungs): The centroid value for this cluster is 0.189932, indicating the central tendency of features in chest X-ray images depicting Pneumonia affected lungs.
- 4. Cluster 3 (Normal Lungs): This cluster is characterized by a centroid value of 0.239203, suggesting the average features of chest X-ray images portraying normal, healthy lungs.

3.6. Testing Process

All the data analyzed both have their own name labels so that the testing process can be easily carried out. The testing process is carried out by seeing whether the value of the number of white pixels in the test image belongs to the predetermined clustering class. The results can be seen in the table 16. The testing process can be carried out in several steps as follows:

p-ISSN: 2528-1682 e-ISSN: 2527-9165

- 1. Grouping data for each category in the cluster class and match the value of the calculation of the previous ratio with the predetermined centroid point.
- 2. Count the amount of data for each category that is correctly included in the clustering class according to its name label.

		1 abic 1	6. Result of The Cluste	51	
	Classes	Actual Class			
	Classes	Covid-19	Tuberculosis	Pneumonia	Normal
ss	Covid-19	73	12	9	13
ed Class	Tuberculosis	56	521	42	32
Predicted 	Pneumonia	20	11	702	19
Į –	Normal	126	112	116	988

Table 16. Result of The Cluster

3.7. Result of Model Validation Test

The table shows that the number of data labeled Covid-19 that is correctly included in the Covid-19 lung cluster class is as much as the total data, the amount of data labeled as Tuberculosis that is correctly included in the Tuberculosis lung cluster class is as much as the total data, the amount of data labeled Pneumonia that is correctly included in the Pneumonia lung cluster class as much as the total data, and the number of data labeled Normal that is correctly included in the Normal lung cluster class as much as the total data.

The validation test is carried out with equation (4) [12] and shows that the results of the accuracy of applying the K-Means Clustering method to Chan-Vese and Canny Edge-Based Image Segmentation are 80%.

Accuracy =
$$\frac{\text{The Number of Clustered Data That Corresponds To The Data Label}}{\text{Total}} \times 100\% = \frac{2284}{2852} \times 100\% = 80\%$$
 (4)

5. CONCLUSION

The findings of this study reveal that the application of the K-Means Clustering method to images resulting from Chan-Vese segmentation and Canny Edge Detection yields an overall accuracy of 80%. This accuracy is computed by assessing the alignment of the data in the cluster class with its corresponding data label. However, it is crucial to acknowledge that several factors can influence this result, with the quantity of data being a notable one. The accuracy is intricately linked to the dataset size, and obtaining a higher or lower accuracy level is contingent on factors beyond just employing the right methodology.

In delving deeper into the observed results, it becomes evident that while the chosen methods—Chan-Vese segmentation and Canny Edge Detection—have demonstrated a commendable accuracy, there exists potential for improvement. Further research avenues could explore the application of alternative segmentation and edge detection methods. Investigating the effectiveness of cutting-edge techniques or hybrid approaches might contribute to enhanced accuracy, especially in detecting more complex lung diseases.

For future studies, researchers might also consider varying the quantity of data used for analysis. A comprehensive investigation with an increased dataset size could provide a more nuanced understanding of the methodology's performance. Balancing the right method with an optimal amount of data holds the potential to yield more accurate and robust results.

Additionally, it would be valuable to extend this research to encompass a broader spectrum of lung diseases, including those of a more intricate nature. Exploring diverse datasets with varying complexities could further validate and generalize the applicability of the clustering method, thereby contributing to advancements in the field of lung disease detection.

REFERENCES

- [1] Niederman, M. S., & Cilloniz, C. (2022). Aspiration pneumonia. Revista Espanola de Quimioterapia, 35. https://doi.org/10.37201/req/s01.17.2022
- [2] Smithard, D. G., & Yoshimatsu, Y. (2022). Pneumonia, Aspiration Pneumonia, or Frailty-Associated Pneumonia? Geriatrics (Switzerland), 7(5). https://doi.org/10.3390/geriatrics7050115
- [3] Natarajan, A., Beena, P. M., Devnikar, A. V., & Mali, S. (2020). A systemic review on tuberculosis. In Indian Journal of Tuberculosis (Vol. 67, Issue 3). https://doi.org/10.1016/j.ijtb.2020.02.005
- [4] Kiani, D. (2023). X-Ray Diffraction (XRD). In Springer Handbooks. https://doi.org/10.1007/978-3-031-07125-6_25
- [5] Patil, B. M., & Burkpalli, V. (2022). Segmentation of cotton leaf images using a modified chan vese method. Multimedia Tools and Applications, 81(11). https://doi.org/10.1007/s11042-022-12436-8
- [6] Song, J., Pan, H., Liu, W., Xu, Z., & Pan, Z. (2021). The Chan-Vese Model with Elastica and Landmark Constraints for Image Segmentation. IEEE Access, 9. https://doi.org/10.1109/ACCESS.2020.3047848
- [7] Wang, Z., Wang, K., Yang, F., Pan, S., & Han, Y. (2018). Image segmentation of overlapping leaves based on Chan-Vese model and Sobel operator. Information Processing in Agriculture, 5(1). https://doi.org/10.1016/j.inpa.2017.09.005
- [8] Zheng, D., Bao, C., Shi, Z., Ling, H., & Ma, K. (2022). Unsupervised Deep Learning Meets Chan-Vese Model. CSIAM Transactions on Applied Mathematics, 3(4). https://doi.org/10.4208/csiam-am.SO-2021-0049
- [9] Sekehravani, E. A., Babulak, E., & Masoodi, M. (2020). Implementing canny edge detection algorithm for noisy image. Bulletin of Electrical Engineering and Informatics, 9(4). https://doi.org/10.11591/eei.v9i4.1837
- [10] Pradeep Kumar Reddy, R., & Nagaraju, C. (2019). Improved canny edge detection technique using S-membership function. International Journal of Engineering and Advanced Technology, 8(6). https://doi.org/10.35940/ijeat.E7419.088619
- [11] Huang, M., Liu, Y., & Yang, Y. (2022). Edge detection of ore and rock on the surface of explosion pile based on improved Canny operator. Alexandria Engineering Journal, 61(12). https://doi.org/10.1016/j.aej.2022.04.019
- [12] Pratiwi, E. H., & Juniati, D. (2022). CLUSTERING OF LUNG DISEASE BASED ON CHEST X-RAY USING DIMENSIONS FRACTAL BOX COUNTING AND K-MEDOIDS. Jurnal Riset Dan Aplikasi Matematika (JRAM), 6(1), 1–12. https://doi.org/10.26740/JRAM.V6N1.P1-12
- [13] Bookstaver, M. (2021). Secondary Data Analysis. In The Encyclopedia of Research Methods in Criminology and Criminal Justice: Volume II: Parts 5-8. https://doi.org/10.1002/9781119111931.ch107
- [14] Ferreira, W. D., Ferreira, C. B. R., da Cruz Júnior, G., & Soares, F. (2020). A review of digital image forensics. Computers and Electrical Engineering, 85. https://doi.org/10.1016/j.compeleceng.2020.106685
- [15] Sundani, D., Widiyanto, S., Karyanti, Y., & Wardani, D. T. (2019). Identification of image edge using quantum canny edge detection algorithm. Journal of ICT Research and Applications, 13(2). https://doi.org/10.5614/itbj.ict.res.appl.2019.13.2.4
- [16] Sinaga, K. P., & Yang, M. S. (2020). Unsupervised K-means clustering algorithm. IEEE Access, 8. https://doi.org/10.1109/ACCESS.2020.2988796
- [17] Rao, B. S. (2020). Dynamic Histogram Equalization for contrast enhancement for digital images. Applied Soft Computing Journal, 89. https://doi.org/10.1016/j.asoc.2020.106114
- [18] Baskar, A., Rajappa, M., Vasudevan, S. K., & Murugesh, T. S. (2023). Digital Image Processing. In Digital Image Processing. https://doi.org/10.1201/9781003217428
- [19] Agrawal, S., Panda, R., Mishro, P. K., & Abraham, A. (2022). A novel joint histogram equalization based image contrast enhancement. Journal of King Saud University Computer and Information Sciences, 34(4). https://doi.org/10.1016/j.jksuci.2019.05.010

Enchancing Lung Disease Classification through K-Means Clustering, Chan-Vese Segmentation, and Canny Edge Detection on X-Ray Segmented Images

by Joko Riyanto

Submission date: 06-Nov-2025 11:37AM (UTC+0700)

Submission ID: 2805088658 **File name:** 1. JOIN.pdf (605.84K)

Word count: 6030 Character count: 31044



JOIN (Jurnal Online Informatika)

p-ISSN: 2528-1682, e-ISSN: 2527-9165 Volume 9 Number 1 | June 2024: 89-99 DOI: 10.15575/join.v9i1.1178

Enchancing Lung Disease Classification through K-Means Clustering, Chan-Vese Segmentation, and Canny Edge Detection on X-Ray Segmented Images

Joko Riyono¹, Christina Eni Pujiastuti², Sofia Debi Puspa³, Supriyadi⁴, Fayza Nayla Riyana Putri⁵

1.2.3.4 Fakultas Teknologi Industri, Universitas Trisakti, Jakarta

5 Information System, Universitas Diponegoro, Semarang

Article Info

Article history:

Received September 02, 2023 Revised February 15, 2024 Accepted April 21, 2024 Available Online May 06, 2024

Keywords:

Canny Chan-Vese K-Means Clustering Lungs Segmentation X-Ray Image

BSTRACT

The lungs are one of the vital organs in the human body. Not only play a file in the respiratory system, the lungs are also responsible for the man circulatory system. Supporting examinations can also facilitate tedical workers in determining the diagnosis. Usually a lung amination is complemented by a chest X-ray examination procedure. This examination aims to see directly and assess the severity of lung conditions. With current technological advances, image analysis can be done easily. Through digital image processing methods, information can be obtained from images that can be used for analysis as a support for diagnoses in the world of health. Image segmentation is a method in which digital images are divided into several segments or subgroups based on the characteristics of the pixels in the image. In this study, clustering with the K-Means method will be carried out on the results of segmentation of x-ray images of lung diseases, namely Covid-19. Tuberculosis, and Pneumonia. The segmentation method that will be implemented is the Chan-Vese Method and the Canny Edge Detection Method. This research shows that the results of the accuracy of applying the K-Means Clustering method to Chan-Vese and Canny Edge-Based Image Segmentation are 80%.

Corresponding Author:

loko Rivono.

Fakultas Teknologi Industri, Universitas Trisakti, Jakarta, Indonesia. Email: jokoriyono@trisakti.ac.id

1. INTRODUCTION

The lungs are one of the vital organs in the human body. Not only play a role in the respiratory system, the lungs are also responsible for the human circulatory system. Lung health can be influenced by many factors such as lifestyle, environmental hygiene, and heredity [1]. If there is a malfunction in the lungs, human health will be disrupted as a whole. Therefore, examination of lung malfunction should be done as early as possible.

The procedure carried out in a lung examination usually requires investigations because lung diseases generally have similar symptoms such as coughing, fever, decreased body weight, loss of appetite, and so on [2]. Supporting examinations can also facilitate medical workers in determining the diagnosis. Usually a lung examination is complemented by a chest X-ray examination procedure [3]. This examination aims to see directly and assess the severity of lung conditions.

The chest X-ray procedure provides an image based on the diffraction of electromagnetic waves, namely X-rays. The use of this light makes it possible to see human organs visually without having to do a surgical procedure (non-invasive procedure). This procedure produces a two-dimensional image as a representation of the condition of the lungs in the human body and basically this examination is only done through visual observation [4]. Therefore, of course, proper analysis is needed in determining the diagnosis through chest X-ray images.

With current technological advances, image analysis can be done easily. Through digital image processing methods, information can be obtained from images that can be used for analysis as a support for diagnoses in the world of health. Of course, this can also be applied to chest x-ray images.

Digital image processing is one of the areas of research in computer science. Broadly speaking, digital image processing works by analyzing digital images in such a way as to obtain a more perfect image. Not only that, image processing in research is also used in extracting information on images as needed. To extract information on several parts of an image, it is usually done with the segmentation method first.

Basically, the segmentation method is used to separate objects in an image. Image segmentation works by dividing digital images into several segments based on the characteristics of the image. This method allows for the separation of objects from the background. This is of course very necessary in research elated to image analysis to extract or obtain information from the desired parts of the image.

Image segmentation is a method in which digital images are divided into several segments or subgroups based on the characteristics of the pixels in the image [5]. This aims to reduce the detector's inference time when processing the entire image because with segmentation, the detector does not need to process the entire image but only the region selected by the segmentation algorithm. Image segmentation aims to classify areas that have similarities so that they can also distinguish objects in the image from their background [6].

There are two segmentation techniques that are often used and can be divided into two categories, namely Region Segmentation which is a segmentation technique to find regions that meet certain homogeneity criteria such as finding color values that have similarities with other pixels so that they can be used as one region and Edge-Based Segmentation which is a technique for finding edges between regions between different characteristics [7].

The Chan-Vese strategy could be a locale division procedure, which could be a strategy that works without borders. The dynamic form show is one of the working models of division procedure that employments vitality and constrain imperatives on the picture into cluster locales [6]. The dynamic form demonstrate is commonly utilized in different picture preparing applications, particularly in therapeutic picture processing such as chest X-ray pictures, brain CT looks or MRI pictures of organs. Positive edge models are utilized in advanced picture preparing by pixel separation. The Chan-Vese strategy is utilized to distinguish visual objects with developmental energies. The advancement of the Mumford-Shah demonstrate and this demonstrate is based on the vitality diminishment issue, which can be re-expressed as equations of unequivocal levels, driving to a less difficult way of understanding the issue [8].

Canny identify is an edge-based division method found by John F.Canny in 1986 [9]. Basically, the Canny strategy works by employing a grayscale picture as input and producing concentrated discontinuities as yield or edge images. In its application, there are steps for shrewd edge location strategy i.e. smooth or channel commotion, calculate incline quality or slope course, apply delay edge prepare setting, not max [10]. This strategy has criteria that moreover ended up its advantage in picture division strategy, specifically Canny Detector has the capacity to distinguish edges based on indicated convolution parameters and is adaptable in decide the level of edge thickness discovery, to supply a least of separate between the edge of the location result and the initial edge, as it were one reaction on each edge to play down clutter within the post-processing step there [11].

Previous research has been carried (7) by Elsha Heny Pratiwi and Dwi Juniandi in 2022 regarding their research entitled Clustering Lung Disease Based on Chest X-Rays Using Fractal Dimensions Box Counting and K-Medoids. In his research, clustering of lung diseases was carried out based on the results of information from x-ray images of the lungs obtained through the canny segment ion method and resulted in an accuracy of 87% [12].

In this study, clustering with the K-Means method will be carried out on the results of segmentation of x-ray images of lung diseases, namely Covid-19, Tuberculosis, and Pneumonia. The segmentation method that will be implemented is the Chan-Vese Method and the Canny Edge Detection Method.

METHOD

This research was conducted through a quantitative approach because the entire process was carried out using data in the form of numbers as an analytical tool. The data in this research is a type of data in the form of images obtained from previous studies. It can be said, the data used in this study is secondary data. Secondary data is data that is already available and collected by other parties outside the agency under study. Secondary data can generally be obtained through websites, books, articles,

Enchancing Lung Disease Classification through K-Means Clustering. Chan-Vese Segmentation, and Canny Edge Detection on X-Ray Segmented Images (Joko Riyono*, Christina Eni Pujiastuti*, Sopia Debi Puspa*, Supriyadi4, Fayza Nayla Riyani Putri*)

internal organizational records and so on [13]. In this study, data was obtained through a site that contains many types of datasets that are commonly used by researchers in conducting research, namely Kaggle.

The image data used as the research subject is an x-ray image of the chest from patients with Covid-19 lung disease, tuberculosis, pneumonia, and healthy lungs which will also be used to extract information from the image in the form of numerical data from the results of segmentated image. This numeric data will be used again in the clustering process to produce disease cluster classes based on the number of white pixel areas in the segmented image. In this study, there are several stages described as a flowchart as shown in Figure 1 below:

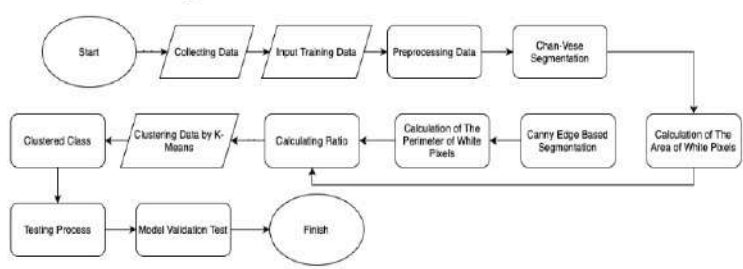


Figure 1. Research Methods Flowchart

The segmentation process applied to the image aims to obtain the features used in the analysis process, in this case, namely the white area in the segmented image [14]. This white area represents the damaged area of the lungs. Before the segmentation process is carried out, the image goes through several two stages in the data preprocessing process, namely the Resize process, Grayscaling Process and the Filtering process with Histogram Equalization.

The image segmentation process is content in the co

Edge detection in an image is a process that produces the edges of an image object, its purpose is to mark the part that becomes a detailed image. Canny edge detection is one of the edge detection algorithms that has a minimum error rate and produces optimal edge images [15]. The edge (edge) is a sudden (large) change in the value of the intensity of gray degrees in a short distance. The purpose of edge detection is to group objects in the image, and is also used to further analyze the image.

The segmentation process, crucia or feature extraction, employed two methods: Chan-Vese and Canny edge detection. The Chan-Vese method, based on curve evolution techniques and Mumford-Shah function, aimed to detect damaged areas in the lungs by focusing on the white regions in segmented images. The Canny edge detection, known for its minimum error rate and optimal edge images, identified sudden changes in intensity, marking detailed parts of the images. Both methods contributed to obtaining precise data on the white pixel area representing lung damage

After the segmentation process is complete, numerical data will be obtained in the form of white pixel area in the image which will then be used in the clustering process to group the data into several classes, namely the Covid-19 class, Tuberculosis, Pneumonia, and Normal or healthy lung class. Mathematically, K-Means clustering is carried out in 4 stages as [16]:

1. Initialize the centroid values randomly

$$v = \frac{\sum_{i=1}^{n} x_i}{n} := 1, 2, 3, ...n$$
 (1)

Information:

v: centroid on cluster

x_i: i-th object

n : numbe(5)f objects/number of cluster member objects.

Place each data point to the nearest centroid by calculating the distance of each data point to the centroid in Euclidean distance

$$(x,y) = ||x-y|| = \sqrt{\sum_{i=1}^{n} (x_i - y_i)^2} \cdot i = 1,2,3,...n$$
 (2)

Information :

xi: ith x object

yi : y-th power

n: number of objects

- Recalculate the centroid of the newly formed cluster by calculating the mean of each data point in the cluster.
- 4. Perform optimization to meet the criteria by repeating the last two steps.

The research strategy systematically applied these methods, and testing procedures involved applying the segmentation methods to chest X-ray images, extracting numerical data, and using K-Means clustering to classify diseases and healthy lungs based on the white pixel area in the segmented image. The research incorporated a robust testing process to evaluate the effectiveness of the applied methodologies. Each dataset was labeled with respective class names, facilitating the testing process. The assessment involved comparing the number of white pixels in test images to predetermined clustering classes.

3. RESULT AND DISCUSSION

The first stage in this study was to collect x-ray image data used as objects in this study. Data in the form of digital data will be processed in the Joint Photographic Experts Group (*jpeg) format. The x-ray image data used is x-ray data including Covid-19 disease, Tuberculosis, Pneumonia and healthy base.

No.	Class	Total Data
1	Covid-19	107
2	Tuberculosis	651
3	Pneumonia	752
4	Normal Lungs	1342

In table 1, there are types and amounts of data used in this research process. All data is collected through the Kaggle website which provides various kinds of datasets for research purposes. This data is obtained by downloading the required dataset.

The next step is image preprocessing. The image epreprocessing stage goes through three stages which aim to improve the quality of the raw data (image) before further analysis. These three stages are resizing all image sizes to 256x256 pixels so that all images are the same size, changing all RGB images to Grayscaling images, and carrying out the filtering process with the Histogram Equalization Method.

3.1. Preprocessing Process

3.1.1. Image Resizing Process

The normalization process in the image aims to change the size of the image resolution so that all images have the same resolution size. Changes in the size of the image resolution will be equated to 256×256 pixels. With a size of 256×256 pixels, the image size can be represented as a matrix with 256 rows and 256 columns. Image size normalization process is done by imresize function via MATLAB. This process will display an image with a size of 256×256 as shown below:



Figure 2. Resize Image

3.1.2. Grayscalling Image Process

The grayscaling process in the image aims to change the RGB (Red, Green, Blue) image to a grayscale image with an intensity of 0 to 255 (8-bit image). The grayscalling process in MATLAB is done with the function rgb2gray. The results of this stage can be seen in the Figure 3 below:



Figure 3. Grayscalling Image

3.1.3. Filtering Image Process With Histogram Equalization

Filtering process aims to improve image quality by reducing noise and adjusting image brightness. The filtering process in this research uses the Histogram Equalization method, which is a graphic equalization that represents the distribution of grayscale image intensities [19]. The filtering process in this study uses the Histogram Equalization technique, which is a graphic equalization process that represents the distribution of grayscale image intensities [17]. This process is done with the histeq function in MATLAB. The image on the right from Figure 5 shows that the image already has better contrast and a flatter histogram than Figure 4.

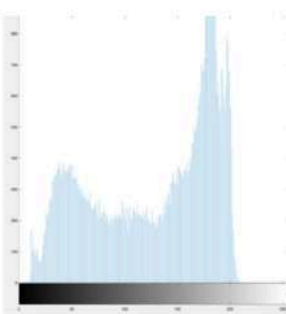


Figure 4. Before Filtering

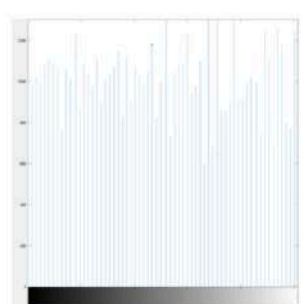


Figure 1. After Filtering

3.2. Calculation Process of The White Area of The Chan-vese Segmentation Image

The normalization process in the image aims to change the size of the image resolution so that all images have the same resolution size. Changes in the size of the image resolution will be equated to 256×256 pixels. With a size of 256×256 pixels, the image size can be represented as a matrix with 256×256 columns [18]. Image size normalization process is done by imresize function via MATLAB. This process will display an image with a size of $256 \times 256 \times 256$ as shown below:



Figure 6. Initialization Mask

The segmentation process using the Chan-Vese method will produce black and white images as shown in Figure 7 which is a comparison of the images before and after segmentation.

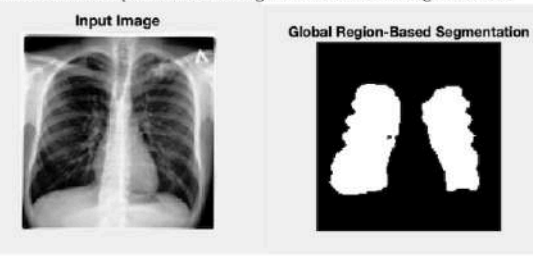


Figure 7. Comparison of Raw and Segmented Image

The next step is to convert the segmented image into a binary image with the im2bw function and fill in imperfect image areas that have holes with the imfill function. After everything has been done, the calculation of the area of white pixels in the image can be done with the regionprops function, which is a function in Matlab that is used to measure the properties of a binary image. Data on the area of white pixels in segmented images can be seen in Table 2 for Covid-19, Table 3 for Tuberculosis, Table 4 for Pneumonia, Table 5 for Normal Lungs.

Table 2. Area of White Pixels of Covid-19 Image

No.	Data	Area
1	'COVID19(460) Small.jpeg'	2060
2	'COVID19(461) Small.jpeg'	2070
3	'COVID19(462) Small.jpeg'	2313
4	'COVID19(463) Small.jpeg'	2416
5	'COVID19(464) Small.jpeg'	3384

Table 3. Area of White Pixels of Tuberculosis Image

No.	Data	Area	_
1	"Tuberculosis-1 Small.jpeg"	4326	
2	"Tuberculosis-10 Small.jpeg"	3676	
3	"Tuberculosis-100 Small.jpeg"	4255	
4	"Tuberculosis-101 Small.jpeg"	4462	
5	"Tuberculosis-102 Small.jpeg"	3340	

Enchancing Lung Disease Classification through K-Means Clustering, Chan-Vese Segmentation, and Canny Edge Detection on X-Ray Segmented Images (Joko Riyono', Christina Em Pujiastuti', Sopia Debi Puspa', Supriyadi4, Fayza Nayla Riyani Putri')

Table 4. Area of White Pixels of Pneumonia Image

No.	Data	Area
1	'person1000_2931.jpeg'	3320
2	'person1000_1681.jpeg'	2040
3	'person1000_2932.jpeg'	1799
4	'person1000_2932.jpeg'	1761
5	'person1000_2934.jpeg'	3039
	Table 5. Area of White Pixels of No	rmal Lungs Image
o.	Data	Area
1	'[M-0115-0001.jpeg'	2194
2 3	'IM-0117-0001.jpeg'	1842
3	'IM-0119-0001.jpeg'	1732
4	'IM-0122-0001 ineg'	2010

3.3. Calculation Process of The White Area of The Canny Edge-Based Segmentation Image

The next image segmentation process uses the second method, namely Canny Edge Detection. With this process, we will find a border around the chan-vese segmented image by detecting changes in brightness levels and generating the circumference of the image as another variable needed in the clustering process.

This segmentation process uses the edge function in Matlab. By using the edge function, an image of the Canny edge detection results will be obtained as shown in Figure 9 below.

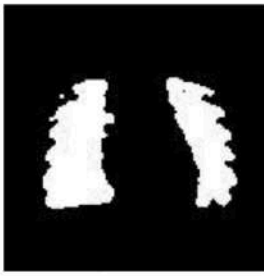


Figure 8. Chan-Vese Segmentation

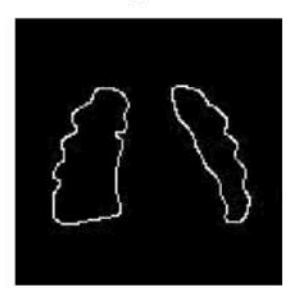


Figure 9. Canny Segmentation

Through the image segmentation results from Chan-Vese and then Canny, we get the circumference of the edge that surrounds the image. The results are described in the Table 6 for Covid-19, Table 7 for Tuberculosis, Table 8 for Pneumonia, Table 9 for Normal Lungs.

No.	Data	Circumference
1	'COVID19(460) Small.jpeg'	499
2	'COVID19(461) Small.jpeg'	401
3	'COVID19(462) Small.jpeg'	376
4	'COVID19(463) Small.jpeg'	431
F	ACCOMBINATORACE AN Control History	446

Table 7. White Pixels Circumference of Tuberculosis Image

No.	Data	Circumference
1	'Tuberculosis-1 Small.jpeg'	484
2	"Tuberculosis-10 Small.jpeg"	480
3	"Tuberculosis-100 Small.jpeg"	474
4	'Tuberculosis-101 Small.jpeg'	492
5	"Tuberculosis-102 Small.jpeg"	479

Table 8. White Pixels Circumference of Pneumonia Image

No.	Data	Circumference
1	'person1000_2931.jpeg'	586
2	'person1000_1681.jpeg'	382
3	'person1000_2932.jpeg'	394
4	'person1000_2932.jpeg'	399
5	'person1000_2934.jpeg'	346

Table 9 White	Pixels Circumfereno	of Normal	Lungs Image

No.	Data	Circumference
1	'IM-0115-0001.jpeg'	491
2	'IM-0117-0001.jpeg'	498
3	'IM-0119-0001.jpeg'	468
4	'IM-0122-0001.jpeg'	397
5	'IM-0125-0001.jpeg'	491

3.4. Calculating Ratio

So far, area and circumference data have been obtained from the segmented image. Furthermore, ratio calculations are carried out because the size of human lungs has different sizes. With this step, the data can be used for the next clustering process.

This process is done by the equation (3). For example, one of the data calculations for the Covid-19 data below:

- Number of White Pixel (Canny Edge-Based Segmentation) of "COVID19(460) Small.jpeg": 491
- Number of White Pixel (Chan-Vese Segmentation) of "COVID19(460) Small.jpeg": 2060

Calculation:
$$\frac{\text{The Number of Pixels of The Canny Detection Segmented Image}}{\text{The Number of Pixels of The Chan-Vess Segmented Image}} = \frac{491}{2060} = 4,12825651$$
 (3)

From the calculation results above, it can be concluded that the number of white pixels in the "COVID19(460) Small, jpeg" image is 4.12825651. The same process applies to all images and the results are as shown in the table below, The research involved a detailed analysis of various medical images, and the results are presented in Tables 10 to 13, showcasing the white pixel ratios for different categories of lung images. Each table provides specific details for the examined images, including the file names, circumference, area, and the calculated white pixel ratio.

Table 10. White Pixels Ratio of Covid-19 Image

No.	Data	Circumference	Area	Ratio
1	'COVID19[460] Small.jpeg'	499	2060	0,24223301
2	'COVID19(461) Small.jpeg'	401	2070	0,19371981
3	'COVID19[462] Small.jpeg'	376	2313	0,16255945
4	'COVID19(463) Small.jpeg'	431	2416	0,17839404
5	'COVID19(464) Small.jpeg'	446	3384	0,13179669

Table 10 outlines the white pixel ratios for several Covid-19 chest X-ray images. Each entry includes the file name, circumference, area, and the calculated ratio. For instance, 'COVID19(460) Small.jpeg' has a circumference of 499, an area of 2060, and a calculated ratio of 0.24223301

Table 11. White Pixels Ratio of Tuberculosis Image

No.	Data	Circumference	Area	Ratio
1	"Tuberculosis-1 Small.jpeg"	484	4326	0,11188165
2	"Tuberculosis-10 Small.jpeg"	480	3676	0,19371981
3	'Tuberculosis-100 Small.jpeg'	474	4255	0,16255945
4	'Tuberculosis-101 Small.jpeg'	492	4462	0.17839404
5	'Tuberculosis-102 Small.ipeg'	479	3340	0.13179669

In Table 11, the white pixel ratios for Tuberculosis chest X-ray images are presented. Similar to Table 10, it includes file names, circumference, area, and the calculated ratio. For example, "Tuberculosis-1 Small.jpeg" has a circumference of 484, an area of 4326, and a calculated ratio of 0.11188165.

Table 12. White Pixels Ratio of Pneumonia Image

No.	Data	Circumference	Area	Ratio
1	'person1000_2931.jpeg'	586	3320	0,17650602
2	'person1000_1681.jpeg'	382	2040	0,19371981
3	'person1000_2932.jpeg'	394	1799	0,16255945
4	'person1000_2932.jpeg'	399	1761	0.17839404
5	'person1000_2934.jpeg'	346	3039	0,13179669

Enchancing Lung Disease Classification through K-Means Clustering, Chan-Vese Segmentation, and Canny Edge Detection on X-Ray Segmented Images (Joko Riyono', Christina Eni Pujiastuti's, Sopia Debi Puspa', Supriyadi4, Fayzo Nayla Riyani Putri's)

Table 12 provides information on the white pixel ratios for Pneumonia chest X-ray images. Each entry includes the file name, circumference, area, and the calculated ratio. 'person1000_2931.jpeg' has a circumference of 586, an area of 3320, and a calculated ratio of 0.17650602, as an example

Table 13. White Pixels Ratio of Normal Lungs Image

No.	Data	Circumference	Area	Ratio
1	'IM-0115-0001.jpeg'	491	2194	0,22379216
2	'IM-0117-0001.jpeg'	498	1842	0,27035831
3	'IM-0119-0001.jpeg'	468	1732	0,27020785
4	'IM-0122-0001.jpeg'	397	2010	0,19751244
5	'IM-0125-0001.ipeg'	491	1787	0.27476217

The white pixel ratios for images of normal lungs are detailed in this table. It includes file names, circumference, area, and the calculated ratio. 'IM-0115-0001.jpeg' has a circumference of 491, an area of 2194, and a calculated ratio of 0.22379216, as one example. These tables collectively provide a comprehensive overview of the white pixel ratios across different types of chest X-ray images, contributing valuable insights into the characteristics of each category.

3.5. Clustering Data by K-Means

After all image processing has been completed, the next step is the clustering process using the K-Means method. This process begins by calculating the average of all data including data on the ratio of Covid-19, Tuberculosis, Pneumonia, and Healthy Lungs. The average value is obtained with the data from the previous ratio calculation process.

Table 14. Mean Value Data

No.	Data	Average (Mean)
1	Covid-19 Lungs	0.16540681
2	Tuberculosis Lungs	0.10936217
3	Pneumonia Lungs	0.2004141
4	Normal Lungs	0.24035373

As in the table 14, you can see the average of each disease data. This clustering process is carried out so that four cluster classes are obtained, namely Cluster 0, Cluster 1, Cluster 2, Cluster 3. Determining the name of the cluster is done by finding the value that is closest to the average in the data for each disease. Cluster 0 has the closest value to the average value in the Covid-19 data, as well as Cluster 1 for Tuberculosis data, Cluster 2 for Pneumonia data, Cluster 3 for Normal Lung data. The clustering process is carried out using the Jupyter Notebook software and the cluster results and centroid values are shown in the table below:

Table 15. Centroid for Each Cluster

No.	Cluster	Centroid
1	Cluster 0 (Covid-19 Lungs)	0.154021
2	Cluster 1 (Tuberculosis Lungs)	0.083526
3	Cluster 2 (Pneumonia Lungs)	0.189932
4	Cluster 3 (Normal Lungs)	0.239203

The clustering process was executed using the Jupyter Notebook software, a popular tool for interactive and collaborative data analysis. The results of this process, including the identified clusters and their corresponding centroid values, are summarized in Table 15. This table elucidates the outcomes of the clustering process, showcasing the centroids for each identified cluster. The clusters are differentiated based on the types of lung conditions:

- Cluster 0 (Covid-19 Lungs): The centroid value for this cluster is 0.154021, representing the average position of data points within the cluster. This centroid is indicative of the characteristics associated with chest X-ray images depicting Covid-19 affected lungs.
- Cluster 1 (Tuberculosis Lungs): With a centroid value of 0.083526, this cluster represents the average features of chest X-ray images illustrating Tuberculosis affected lungs.
- Cluster 2 (Pneumonia Lungs): The centroid value for this cluster is 0.189932, indicating the central tendency of features in chest X-ray images depicting Pneumonia affected lungs.
- Cluster 3 (Normal Lungs): This cluster is characterized by a centroid value of 0.239203, suggesting the average features of chest X-ray images portraying normal, healthy lungs.

3.6. Testing Process

All the data analyzed both have their own name labels so that the testing process can be easily carried out. The testing process is carried out by seeing whether the value of the number of white pixels in the test image belongs to the predetermined clustering class. The results can be seen in the table 16. The testing process can be carried out in several steps as follows:

Grouping data for each category in the cluster class and match the value of the calculation of the
previous ratio with the predetermined centroid point.

previous ratio with the predetermined centroid point.Count the amount of data for each category that is correctly included in the clustering class according to its name label.

Table 16. Result of The Cluster

	Classes		Actual (lass	
		Covid-19	Tuberculosis	Pneumonia	Normal
	Covid-19	73	12	9	13
-	Tuberculosis	56	521	42	32
	Pneumonia	20	11	702	19
-	Normal	126	112	116	988

3.7. Result of Model Validation Test

The table shows that the nure of the total data, the amount of date data, the amount of date data, the amount of date data, the amount of data data data, the amount of data data data, and the number of data labeled Normal that is correctly included in the Pneumonia lung cluster class as much as the total data, and the number of data labeled Normal that is correctly included in the Normal lung cluster class as much as the total data.

The validation test is carried out with equation (4) [12] and shows that the results of the accuracy of applying the K-Means Clustering method to Chan-Vese and Canny Edge-Based Image Segmentation are 80%.

$$Accuracy = \frac{\text{The Number of Glustered Data That Corresponds To The Data Label}}{\text{Total}} \times 100\% = \frac{2284}{2852} \times 100\% = 80\% \quad \text{(4)}$$

5. CONCLUSION

The findings of this study reveal that the application of the K-Means Clustering method to images resulting from Chan-Vese segmentation and Canny Edge Detection yields an overall accuracy of 80%. This accuracy is computed by assessing the alignment of the data in the cluster class with its corresponding data label. However, it is crucial to acknowledge that several factors can influence this result, with the quantity of data being a notable one. The accuracy is intricately linked to the dataset size, and obtaining a higher or lower accuracy level is contingent on factors beyond just employing the right methodology.

In delving deeper into the observed results, it becomes evident that while the chosen methods— Chan-Vese segmentation and Canny Edge Detection—have demonstrated a commendable accuracy, there exists potential for improvement. Further research avenues could explore the application of alternative segmentation and edge detection methods. Investigating the effectiveness of cutting-edge techniques or hybrid approaches might contribute to enhanced accuracy, especially in detecting more complex lung diseases.

For future studies, researchers might also consider varying the quantity of data used for analysis. A comprehensive investigation with an increased dataset size could provide a more nuanced understanding of the methodology's performance. Balancing the right method with an optimal amount of data holds the potential to yield more accurate and robust results.

Additionally, it would be valuable to extend this research to encompass a broader spectrum of lung diseases, including those of a more intricate nature. Exploring diverse datasets with varying complexities could further validate and generalize the applicability of the clustering method, thereby contributing to advancements in the field of lung disease detection.

REFERENCES

- [1] Niederman, M. S., & Cilloniz, C. (2022). Aspiration pneumonia. Revista Espanola de Quimioterapia, 35. https://doi.org/10.37201/req/s0117.2022
- Smithard, D. G. & Yoshimatsu, Y. (2022). Pneumonia, Aspiration Pneumonia, or Frailty-Associated Pneumonia? Geriatrics (Switzerland), 7(5). https://doi.org/10.3390/geriatrics7050115 Natarajan, A., Beena, P. M., Devnikar, A. V., & Mali, S. (2020). A systemic review on tuberculosis. In Indian Journal of
- [3] Tuberculosis (Vol. 67, Issue 3). https://doi.org/10.1016/j.ijtb.2020.02.005
- Kiani, D. (2023). X-Ray Diffraction (XRD). In Springer Handbooks. https://doi.org/10.1007/978-3-031-07125-6_25 Patil, B. M., & Burkpalli, V. (2022). Segmentation of cotton leaf images using a modified chan vese method. Multimedia Tools [5] and Applications, 81(11). https://doi.org/10.1007/s11042-022-12436-8
- Song, J., Pan, H., Liu, W., Xu, Z., & Pan, Z. (2021). The Chan-Vese Model with Elastica and Landmark Constraints for Image Segmentation. IEEE Access, 9. https://doi.org/10.1109/ACCESS.2020.3047848
- [7] Wang, Z., Wang, K., Yang, F., Pan, S., & Han, Y. (2018). Image segmentation of overlapping leaves based on Chan-Vese model and Sobel operator, Information Processing in Agriculture, 5(1). https://doi.org/10.1016/j.inpa.2017.09.005
 Zheng, D., Bao, C., Shi, Z., Ling, H., & Ma, K. (2022). Unsupervised Deep Learning Meets Chan-Vese Model. CSIAM Transactions
- [8] on Applied Mathematics, 3(4). https://doi.org/10.4208/csiam-am.SO-2021-0049
- Sekehravani, E. A., Babulak, E., & Masoodi, M. (2020). Implementing canny edge detection algorithm for noisy image. Bulletin of Electrical Engineering and Informatics, 9(4). https://doi.org/10.11591/eei.v94.1837
- [10] Pradeep Kumar Reddy, R., & Nagaraju, C. (2019). Improved canny edge detection technique using S-membership function.
- International Journal of Engineering and Advanced Technology, 8(6). https://doi.org/10.35940/ijeat.E7419.088619
 [11] Huang, M, Liu, Y, & Yang, Y. (2022). Edge detection of ore and rock on the surface of explosion pile based on improved Canny
- operator. Alexandria Engineering Journal, 61(12). https://doi.org/10.1016/j.aej.2022.04.019 [12] Pratiwi, E. H., & Juniati, D. (2022). CLUSTERING OF LUNG DISEASE BASED ON CHEST X-RAY USING DIMENSIONS FRACTAL
 BOX COUNTING AND K-MEDOIDS. Jurnal Riset Dan Aplikasi Matematika (JRAM), 6(1), 1-12.
- https://doi.org/10.26740/JRAM.V6N1.P1-12 [13] Bookstaver, M. (2021). Secondary Data Analysis. In The Encyclopedia of Research Methods in Criminology and Criminal Justice: Volume II: Parts 5-8. https://doi.org/10.1002/9781119111931.ch107
- [14] Ferreira, W. D., Ferreira, C. B. R., da Cruz Júnior, G., & Soares, F. (2020). A review of digital image forensics. Computers and Electrical Engineering, 85. https://doi.org/10.1016/j.compeleceng.2020.106685
- [15] Sundani, D., Widiyanto, S., Karyanti, Y., & Wardani, D. T. (2019). Identification of image edge using quantum canny edge detection algorithm. Journal of ICT Research and Applications, 13(2). https://doi.org/10.5614/itbj.ict.res.appl.2019.13.2.4
- [16] Sinaga, K. P., & Yang, M. S. (2020). Unsupervised K-means clustering algorithm. IEEE Access, 8. https://doi.org/10.1109/ACCESS.2020.2988796
- [17] Rao, B. S. (2020). Dynamic Histogram Equalization for contrast enhancement for digital images. Applied Soft Computing
- Journal, 89. https://doi.org/10.1016/j.asoc.2020.106114
 [18] Baskar, A., Rajappa, M., Vasudevan, S. K., & Murugesh, T. S. (2023). Digital Image Processing. In Digital Image Processing. https://doi.org/10.1201/9781003217428
- [19] Agrawal, S., Panda, R., Mishro, P. K., & Abraham, A. (2022). A novel joint histogram equalization based image contrast enhancement. Journal of King Saud University - Computer and Information Sciences, 34(4). https://doi.org/10.1016/j.jksuci.2019.05.010

Enchancing Lung Disease Classification through K-Means Clustering, Chan-Vese Segmentation, and Canny Edge Detection on X-Ray Segmented Images

	ALITY REPORT	Terrica IIIages	
1 SIMIL	4% 12% INTERNET SO	1% urces publications	2% STUDENT PAPERS
PRIMAF	RY SOURCES		
1	discovery.research	ner.life	11%
2	Submitted to iGro	up	1 %
3	jurnal.unprimdn.a Internet Source	c.id	<1%
4	infokripto.poltekss	sn.ac.id	<1%
5	Submitted to High Pakistan Student Paper	er Education Comm	nission <1 %
6	Prasetyo Wibowo, Arna Fariza, Ferry Astika Saputra. "The combination of the NDBI and machine learning algorithms to classification the development of urban areas in Surabaya uses Landsat 8 Imagery.", 2023 International Electronics Symposium (IES), 2023 Publication		BI and fication urabaya
7	journal.unesa.ac.id	d	<1%
8	_	ayant Shah. "Optima y piecewise smooth ociated variational	\ \ \ \ \ \ \ \ \ \ \ \ \ \ \ \ \ \ \

problems", Communications on Pure and Applied Mathematics, 1989

Publication

9

Adi Budi Prasetyo, Rizki Wahyudi, Imam Tahyudin, Selvia Ferdiana Kusuma, Luzi Dwi Oktaviana, Azhari Shouni Barkah, Budi Artono. "Comparative Analysis of Image on Several Edge Detection Techniques", TEM Journal, 2023

<1%

Publication

Exclude quotes

On

Exclude matches

< 10 words

Exclude bibliography

Эn

Enchancing Lung Disease Classification through K-Means Clustering, Chan-Vese Segmentation, and Canny Edge Detection on X-Ray Segmented Images

GRADEMARK REPORT	
FINAL GRADE	GENERAL COMMENTS
/100	
PAGE 1	
PAGE 2	
PAGE 3	
PAGE 4	
PAGE 5	
PAGE 6	
PAGE 7	
PAGE 8	
PAGE 9	
PAGE 10	
PAGE 11	